Publications of the Astronomical Society of the Pacific, **119**: 1211–1232, 2007 November

Review

Constraints on Type Ib/c Supernovae and Gamma-Ray Burst Progenitors

Chris L. Fryer,[1,2] Paolo A. Mazzali,[3,4] Jason Prochaska,[5] Enrico Cappellaro,[6] Alin Panaitescu,[7] Edo Berger,[8,9,10] Maurice van Putten,[11] Ed P. J. van den Heuvel,[12] Patrick Young,[13,14] Aimee Hungerford,[2] Gabriel Rockefeller,[2] Sung-Chul Yoon,[12] Philipp Podsiadlowski,[15] Ken'ichi Nomoto,[16] Roger Chevalier,[17] Brian Schmidt,[18] and Shri Kulkarni[19]

Received 2007 September 11; accepted 2007 September 18; published 2007 December 3

ABSTRACT. Although there is strong support for the collapsar engine as the power source of long-duration gamma-ray bursts (GRBs), we still do not definitively know the progenitor of these explosions. Here we review the current set of progenitor scenarios for long-duration GRBs and the observational constraints on these scenarios. Examining these models, we find that single stars cannot be the only progenitor for long-duration GRBs. Several binary progenitors can match the solid observational constraints and also have the potential to match the trends that we are currently seeing in the observations. Type Ib/c supernovae are also likely to be produced primarily in binaries; we discuss the relationship between the progenitors of these explosions and those of the long-duration GRBs.

Online material: color figures

1. INTRODUCTION

Since as early as AD 185, the energetic transients known as supernovae have excited the imagination of mankind (Stephenson & Clark 1976; Chin & Huang 1994). We now believe (and even know for a fact in some cases) that many of these supernovae (Types Ib, Ic, and II) arise from the collapse of massive stars. Theorists have gradually converged on a mechanism that takes the potential energy released in the collapse of a stellar core down to a neutron star and injects energy into the convective region above the neutron star, driving an explosion (see Fryer 2003 for a review). However, the details (including the relevant physics) of this explosion mechanism are far from settled. It is important to remember that "supernova" has a phenomenological definition. Any event that disrupts a star with sufficient violence will be observed as a supernova. One of the biggest uncertainties in determining the explosion mechanism is our understanding, or lack thereof, of the supernova progenitor. Although it is likely that the explosion arises from the collapse of a massive ($\gtrsim 8\ M_{\odot}$) star, the exact nature of the evolution of this progenitor is unknown, especially for Type Ib/c supernovae.

One of the latest developments in the study of explosions from collapsing massive stars has been the discovery of gamma-ray bursts (GRBs). Engines invoking the collapse of massive stars have once again become the favored mechanisms behind a class (the long-soft burst class) of GRBs. Observations of these long-duration bursts, such as the association of GRBs with star-forming galaxies and star formation regions in galaxies (Fruchter et al. 2006), have added support to this model. But the most convincing observational evidence has been the concurrent and cospatial "supernovalike" outbursts associated with GRBs (e.g., SN 1998bw, SN 2003dh). These supernovalike bursts are evidence that the GRB explosion is part of the disruption of a massive star.

This association between GRBs and supernovalike explosions has led to the appearance of a new class of stellar explosion, the so-called hypernova. A number of definitions for hypernovae exist, from the energetic outburst produced by a

[1] Department of Physics, University of Arizona, Tucson, AZ.
[2] Computer, Computational, and Statistical Sciences Division, Los Alamos National Laboratory, Los Alamos, NM.
[3] INAF–Osservatorio Astronomico di Trieste, Trieste, Italy.
[4] Max-Planck-Institut für Astrophysik, Garching bei München, Germany.
[5] University of California Observatories–Lick Observatory, University of California, Santa Cruz, CA.
[6] INAF–Osservatorio Astronomico, Padova, Italy.
[7] Integrated Spectroscopy Resource Division, Los Alamos National Laboratory, Los Alamos, NM.
[8] Observatories of the Carnegie Institution of Washington, Pasadena, CA.
[9] Princeton University Observatory, Princeton, NJ.
[10] Hubble Fellow.
[11] Laser Interferometer Gravitational-Wave Observatory Laboratory, Massachusetts Institute of Technology, Cambridge, MA.
[12] Astronomical Institute Anton Pannekoek, University of Amsterdam, Amsterdam, The Netherlands.
[13] Astronomy Department, University of Arizona, Tucson, AZ.
[14] Applied Physics Division, Los Alamos National Laboratory, Los Alamos, NM.
[15] Department of Astrophysics, University of Oxford, Oxford, UK.
[16] Department of Astronomy and RESCEU, University of Tokyo, Bunkyo-ku, Tokyo, Japan.
[17] Department of Astronomy, University of Virginia, Charlottesville, VA.
[18] Mount Stromlo and Siding Spring Observatory, Canberra, ACT, Australia.
[19] Caltech Optical Observatories, California Institute of Technology, Pasadena, CA.

collapsar (Woosley 1993; Paczyński 1998) to the supernova associated with GRB outbursts.[20] Our definition is a bit broader; we use the term hypernova to denote all explosions that exhibit broad lines in their spectra (Nomoto et al. 2005).[21] With this definition, the "supernovae" associated with GRBs are a subset of the hypernova class.

The relationship between normal supernovae and hypernovae has led to intense discussion, with views ranging from "all supernovae are hypernovae and the current models of supernovae are all wrong" to "hypernovae have nothing to do with the explosions of massive stars." The former interpretation essentially ignored the bulk of the existing supernova observations and has finally been put to rest in the GRB community by comparisons between supernovae and hypernovae (Soderberg et al. 2006a, 2006b). The latter interpretation seems unlikely given how well massive star models fit the observed hypernovae (e.g., Deng et al. 2005; Mazzali et al. 2006; Maeda et al. 2006). We take a more moderate interpretation, assuming that hypernovae are a rare set of massive star explosions with an engine different from the standard supernova model.

Although the evidence suggesting that these explosions are produced inside massive stars continues to grow, we know very little else about the engine behind hypernovae and GRBs. Based primarily on the fact that these explosions are different from "normal" supernovae, theorists have argued that the engine itself must also be different. The leading theory, the collapsar engine (Woosley 1993), suggests that the explosion is produced after the massive star collapses to a black hole. The energy released during accretion of the infalling stellar material onto this black hole provides the energy for the explosion (via neutrino annihilation or a magnetic field transfer mechanism; Narayan et al. 1992). However, this can only occur if the energy does not also accrete onto the black hole. The requirement for GRBs, then, is that the infalling material have sufficient angular momentum to hang up in a disk before accreting.

Unfortunately, hypernovae are rare events (roughly 1000 times less frequent than normal supernovae), and their rarity allows theorists the freedom to devise all manner of exotic formation scenarios for the progenitors of these explosions. In this review, we summarize the wide range of possible progenitors and try to constrain them with the current set of observational data. One clue may be that, so far, all hypernovae (with and without GRB jets) have been classified as Type Ib/c supernovae; i.e., these bursts do not have strong hydrogen lines in their spectra. Indeed, hypernovae do not even have strong helium lines in their spectra, suggesting that the progenitors of these explosions have lost much of their helium layer (we discuss this in more detail in § 3). It may well be that the progenitors of hypernovae are merely a subset of the progenitors of their more common cousins, Type Ib/c supernovae. We review these progenitors as well to better understand the link between supernovae and gamma-ray bursts.

In this review, we focus our studies of GRBs on progenitors of the collapsar engine, but we include variants often neglected in discussions of collapsar progenitors. A wide variety of progenitors has been proposed, each including a set of predictions for characteristics that presumably can be compared to observations. We discuss the progenitors and their characteristics in § 2. Studies of the observed hypernova samples (with and without GRB jets) have produced a number of constraints that have been used to argue for or against certain progenitors. However, it is quite difficult to make definitive observational statements on the current set of progenitor predictions. In § 3, we review the current state of observational constraints. The goal of this review is to draw the attention of theorists to the firm observational constraints and of observers to the firm theoretical predictions to provide a road map for the future that will increase the amount of information in the intersection of these two data sets. We conclude with a review of how current models fare with the existing data.

2. PROGENITORS

2.1. Progenitors for Ib/c Supernovae

One possible picture for the origin of Type Ib/c supernovae is that the progenitors for these explosions are the most massive stars (see Hirschi et al. 2004 and references therein). These stars have very strong winds, which ultimately cause the stars to lose their entire hydrogen envelope and become strong Wolf-Rayet (WR) stars. However, when Heger et al. (2003) studied single stars, they found that very few nonrotating single stars at solar metallicity eject their entire hydrogen envelopes in winds. Figure 1 shows the fraction of collapsing stars that form Type II and Type Ib/c supernovae as a function of metallicity from this Heger et al. (2003) study. The thin lines denote those supernovae that Heger et al. (2003) believed would only produce weak supernovae (based on the analysis of Fryer 1999). Note that single nonrotating stars produce Ib/c supernovae only at metallicities above $0.02\,Z_{\odot}$. But we expect these supernovae to have weak shocks and hence eject very little nickel. Without the high shock temperatures and the radioactive nickel to power the light curve, these supernovae will be dim. Strong Ib/c supernovae are not produced at all until the metallicity rises above solar! This assumes, however, that the explosion is powered by the standard neutrino-driven convection mechanism. An alternate engine (such as a collapsar) may be able to produce bright supernovae from these progenitors.

There are a few caveats to these results. First, these results depend sensitively on the mass-loss rates used and rates can shift along the metallicity axis depending on the values adopted

[20] For a while, Woosley wanted to use the term hypernova to rename pair-instability supernovae.

[21] Note that some hypernovae can have relatively normal explosion energies but are still classified as hypernova based on the broad-line features: e.g., 2006aj (Soderberg et al. 2006a, 2006b).

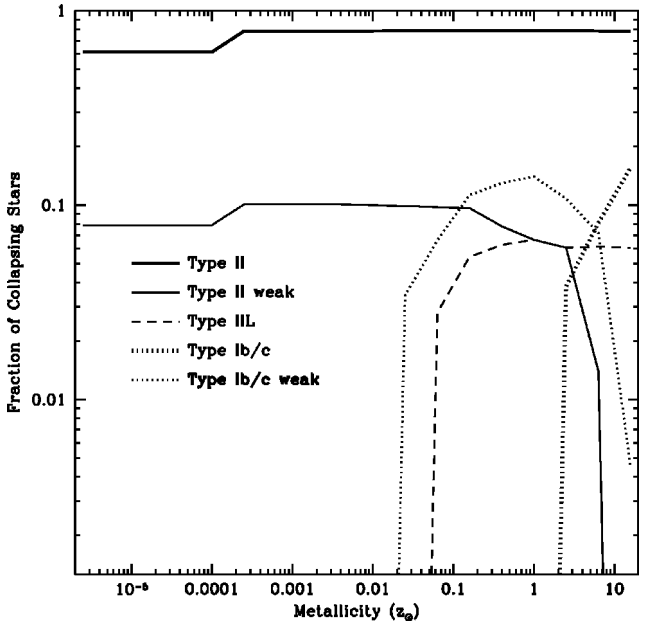

FIG. 1.—Single-star supernova rate as a fraction of total number of collapsing stars as a function of metallicity calculated using the stellar models from Heger et al. (2003). We consider three classes of Type II SNe: normal Type II SNe (Type II), Type II SNe with weak SN explosions (Type II weak), and Type II SNe that have lost most of their hydrogen envelope (Type IIL); and two classes of Type Ib/c SNe: normal Ib/c SNe and weak Ib/c SNe. If single stars dominate the Ib/c rate, these models predict only weak Type Ib/c SNe below solar metallicity.

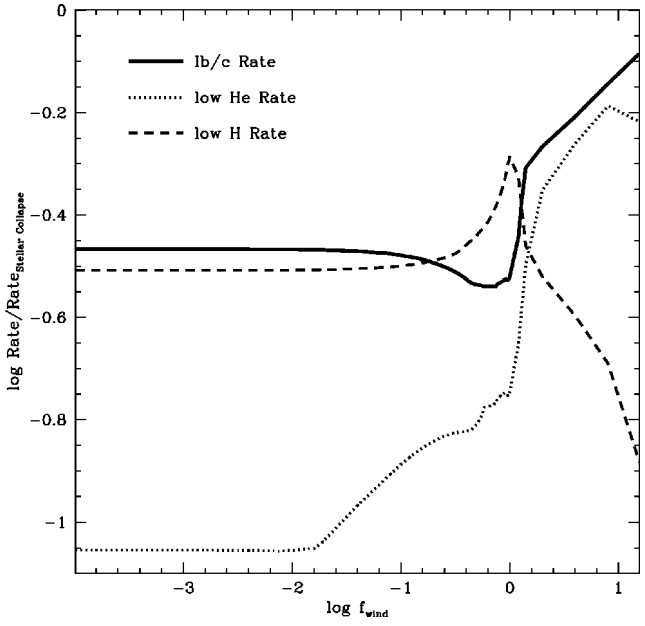

FIG. 2.—Binary-star supernova rate as a function of the mass-loss parameter (see Fryer et al. 1998 for details). We consider three types of SNe: all Type Ib/c SNe, Type Ib/c SNe that have lost more than 1 $M_\odot$ of helium (not necessarily Type Ic SNe, but on their way to becoming Ic SNe), and Type II SNe that have lost $\frac{2}{3}$ of their hydrogen (peculiar Type II or Type IIL SNe) but still retain some hydrogen envelope to be Type II SNe. As the mass-loss parameter increases, the rate of Ib/c and low-helium SNe increases while the rate of low hydrogen (and all Type II SNe for that matter) decreases. This mass-loss parameter can be seen as a parameter for the metallicity. Although the rate of Ib/c SNe is higher at higher mass-loss rates (higher metallicities), it drops less than a factor of 5 when varying the mass-loss parameter from very high mass-loss to essentially no mass-loss rates.

for mass loss. However, if anything, the trend in the last decade has been that early calculations have overestimated the mass loss. Lowering this mass loss would only push the minimum metallicity to form Ib/c supernovae upward. Note also that Yoon & Langer (2005) have found that rapidly rotating stars can mix their hydrogen envelopes, effectively removing the hydrogen envelope by burning it into helium.

Alternatively, these Ib/c supernovae could be formed in binaries (Podsiadlowski et al. 1992; Nomoto et al. 1995a). Mass transfer in binaries can eject matter, forming helium stars (Ib/c progenitors) or stars with peculiar hydrogen envelopes (II pec or II linear, "II-L," progenitors). The list of supernovae that show evidence of a binary companion continues to grow: SN 1987A (Podsiadlowski et al. 1990), SN 1993J (Nomoto et al. 1993; Podsiadlowski et al. 1993; Woosley et al. 1994; Maund et al. 2004), Cas A (Young et al. 2006), SN 2001ig (Ryder et al. 2006), and possibly Puppis A (Winkler et al. 1989) and SN 1994I (Nomoto et al. 1994; Sauer et al. 2006). Given the current uncertainties in stellar evolution, it is difficult to really prove that an observed supernova came from a binary system. With the latest results showing that $\gtrsim$60% (this value could be 100%) of all massive stars are in binaries that will undergo mass transfer (Kobulnicky & Fryer 2007), Type Ib/c are primarily formed in binaries, unless supernovae do not form from massive stars.

Note that Figure 2 also shows the fraction of collapsing stars that lose not only their hydrogen envelopes but also >1 $M_\odot$ of their helium envelopes. This subset of all Type Ib/c supernovae likely have characteristics closer to Type Ic supernovae. Their rate is also sensitive to mass loss (i.e., metallicity); they account for 75% of all Ib/c supernovae at 10 times the Fryer et al. (1998) canonical mass-loss coefficient but less than one-third that total Ib/c rate at lower mass-loss values. For comparison, we also show the rate of supernovae arising from progenitors that have lost 66% of their hydrogen envelopes. These progenitors would produce peculiar or, possibly, linear Type II supernovae.

Assuming that only one-third of all stars are in close, interacting binaries, Podsiadlowski et al. (1992) found that binaries would cause roughly 15% of all stellar collapses to form Ib/c supernovae. With the higher close-binary fraction estimated by Kobulnicky & Fryer (2007), binaries would argue for a rate of strong Type Ib/c supernovae at solar metallicity of roughly

equal to 30% of the total core-collapse supernova rate. Because there are multiple complementary channels that will produce Ib/c supernovae, this estimate is not too dependent on binary parameters (at least in the code used by Podsiadlowski et al. 1992 or Fryer et al. 1998; Kobulnicky & Fryer 2007).

Can we distinguish binary and single-star progenitors? The Type Ib/c supernova rate in binaries does not depend sensitively on the mass-loss rate from winds because the helium star is made during a common-envelope phase. Figure 2 shows the results of the population synthesis code of Fryer et al. (1998), using their standard values for the population synthesis parameters and varying only the mass-loss parameter. The majority of these Type Ib/c supernovae are normal (i.e., not weak/dim) supernovae. Notice that below about $\frac{1}{2}$ solar, the effect of winds on the rate is almost negligible. Varying the wide range of binary population synthesis parameters over modest ranges, we find that the primary uncertainty lies in the choice of initial binary conditions. The Type Ib/c supernova rate depends sensitively on the number of systems with low-mass companions that evolve into common-envelope phases ejecting the hydrogen envelope. Kobulnicky & Fryer (2007) were able to use this result (combined with the latest estimates of the Type Ib/c supernova distribution) to constrain the mass ratio distribution in the observed binaries of the Cygnus OB 2 association. But do these properties change with metallicity? If not, it appears that the binary formation process for Type Ib/c supernovae predicts a very weak dependence on metallicity or redshift.

However, the radial extent of stars does depend on metallicity. Figure 3 shows the radial extent at collapse for several masses as a function of metallicity from the Limongi & Chieffi (2006) stellar models. For binary population synthesis, the maximal extent of the star and the evolutionary period when it achieves this maximal extent are much more important than the final extent. If we assume that these radii are indicative of the relative radius as it evolves in time of these stars, we see that for stars above $\sim$14 $M_{\odot}$, there is a strong dependence on the radius of the star and its initial metallicity. A simple fit to these models yields a scaling factor for this radius ($f_{\rm radius}$) that can vary significantly with metallicity:

$$f_{\rm radius} = 10^{2.0(z-1.0)}, \quad (1)$$

where z is the metallicity of the star in solar units. Such a formula represents an extreme assumption for the evolution of stellar radii. We based it on one code's calculation of the final radius of massive stars and ignored the point from the star showing little metallicity variation. So we have several caveats: this is just one code's result and we know there are variations between codes, the final radii of these stars need not tell us anything about the radius of the star at all times, and finally, even in this result, we had one example where the metallicity dependence was much less extreme. The other limiting extreme would be that the radii of stars do not depend on metallicity whatsoever. Stellar radii are only poorly determined by most codes—predictions between codes can vary by more than a factor of 5 (Fryer et al. 1998). In addition, as we learned with SN 1987A, the radial extent of a star can oscillate. This oscillation is not just determined by the metallicity but also the helium-to-hydrogen ratio (Saio et al. 1988a,1988b). Accurate radii must be calculated as a function of time and then folded into binary calculations to obtain realistic results. And to do this, we must get some agreement in the stellar community.

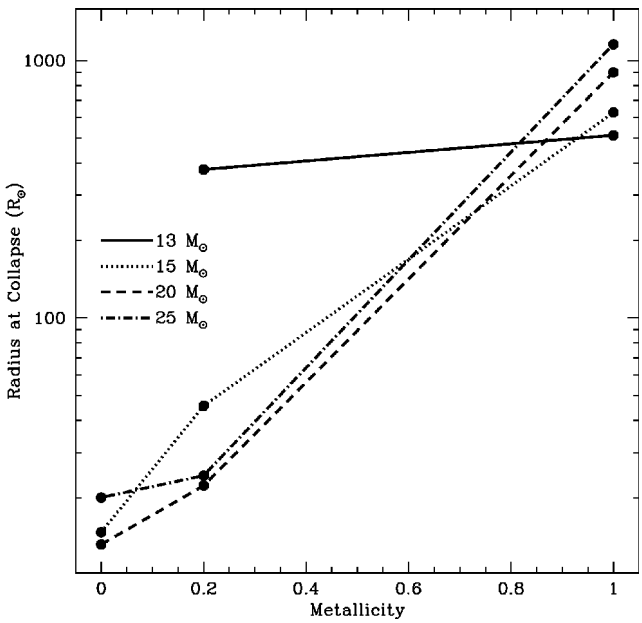

FIG. 3.—Final stellar radii as a function of metallicity for four different mass stars: 13 $M_{\odot}$ (*solid line*), 15 $M_{\odot}$ (*dotted line*), 20 $M_{\odot}$ (*dashed line*), and 25 $M_{\odot}$ (*dot-dashed line*). For most stars, the final radii at zero metallicity are nearly 2 orders of magnitude lower than the final radii at solar metallicity. However, the final radii may not be indicative of the radial extent of stars. For binary population synthesis, the maximal extent of the star and the evolutionary period when it achieves this maximal extent are much more important than the final extent. Currently, errors in stellar evolution codes make it difficult to predict radii to better than a factor of 5 (see Fryer et al. 1998 for a discussion).

But let us assume this extreme case and study its effect on the Type Ib/c supernova rate as a function of metallicity. In this review, we have modified the binary population synthesis code in Fryer et al. (1998) and Kobulnicky & Fryer (2007) to model several grids of binary population synthesis calculations (varying a range of parameters) studying the effects of metallicity and radius scaling factor. A representative set of these models is shown in Figure 4 (this plot consists of 180 population synthesis calculations with 100,000 binaries each corresponding to errors of roughly 1%). Note that the rate of Type Ib/c supernovae drops steeply with decreasing radius. The simulation in this figure assumed a flat mass distribution profile and varied the metallicity and radius factor. Otherwise, the parameters were set to the standard values of Fryer et al. (1998).

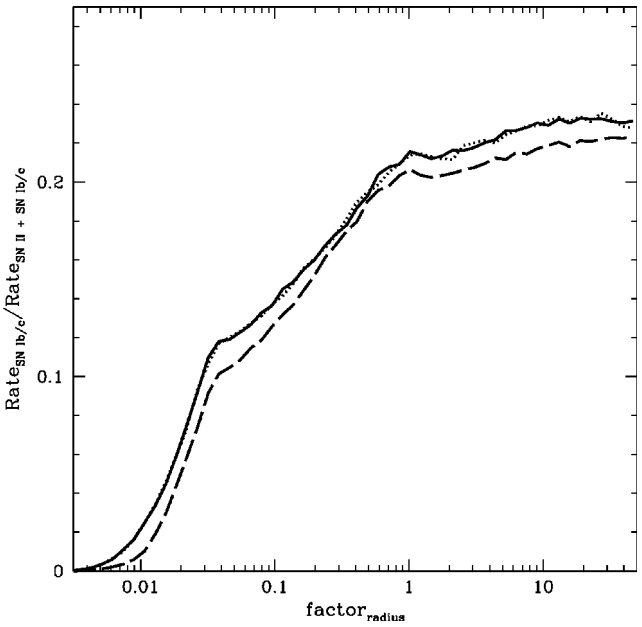

FIG. 4.—Ratio of Type Ib/c SN rate over the total core-collapse SN rate as a function of the multiplicative factor on the radius using the standard set of binary population synthesis parameters and for three different metallicities: solar (*solid line*), 0.1 solar (*dotted line*), and 0.01 solar (*dashed line*). As the radius of the star drops, the binary system does not interact and evolve through a common-envelope phase. Without this phase, the hydrogen envelope is not ejected and the star becomes a Type II, not Type Ib/c SNe.

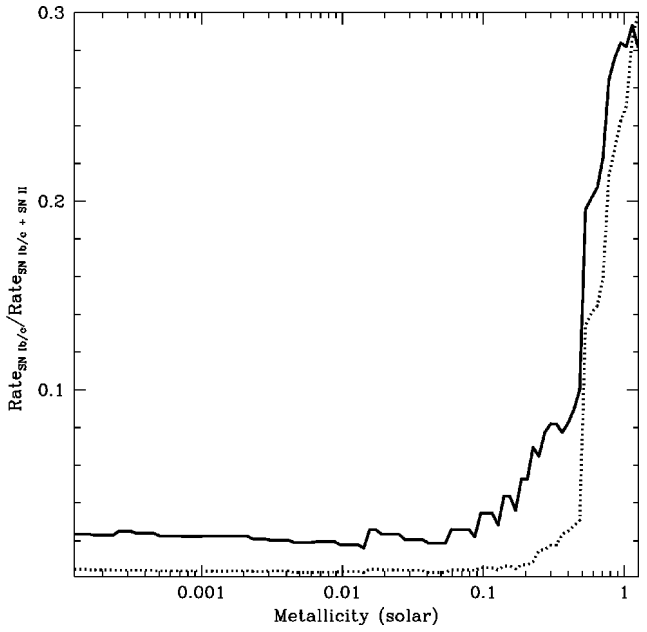

FIG. 5.—Ratio of Type Ib/c SN rate over the total core-collapse SN rate as a function of metallicity for two separate binary population synthesis simulations: standard set of parameters (*solid line*) and an alternate simulation using a high value for the common-envelope efficiency ($\alpha_{CE} = 1.0$) and a Salpeter initial mass function ($\alpha = 2.35$). Both rates drop dramatically below a metallicity of 0.5. By a metallicity of 0.1, the standard model predicts a rate nearly 10 times lower than the value at solar metallicity. For our alternate model, the rate is nearly 100 times lower at the same metallicity.

By modeling a large grid of binary systems (3600 binary population synthesis calculations per grid), we can fold these results into our metallicity-dependent radius from Figure 3 to obtain a metallicity-dependent formation rate for Type Ib/c supernovae (Fig. 5). Figure 5 shows the results of two different grids of binary population synthesis calculations varying the common-envelope efficiency and mass distribution. For both models, there is a sharp drop at a metallicity of roughly 0.5 solar. One model used the standard values for population synthesis (as used in Fig. 3). The Type Ib/c supernova rate drops by over 1 order of magnitude below metallicities of ~ 0.1. The other population synthesis simulation (*dotted line*) was produced from a simulation using a high value for the common-envelope efficiency ($\alpha_{CE} = 1.0$) and a Salpeter initial mass function ($\alpha = 2.35$). For this model, the Type Ib/c supernova rate drops by 2 orders of magnitude by a metallicity of 0.1. If the stellar radii do decrease as much as we assumed, the supernova rate could drop dramatically at higher redshift. However, to determine this for sure, we need more accurate stellar models.

Both single-star and binary-star progenitor scenarios exist for Type Ib/c supernovae. The two major differences in the predictions of these formation scenarios are (1) their relative rates at low metallicity and (2) the predicted number of weak to normal Ib/c supernovae. The single-star mixing model of Yoon & Langer (2005) may change the rate prediction for single stars, but it still predicts that most Ib/c supernovae should produce weak supernova explosions (recall that these weak supernovae are possible GRB progenitors). Figure 6 shows the fate of massive stars (Type Ib/c vs. Type II and normal vs. weak vs. no supernova explosion from the standard supernova mechanism) for the latest grid of mixing models from Yoon et al. (2006). Although this grid of stars, based on Tables 4–7 in Yoon et al. (2006), produces no normal Type Ib/c supernovae, we must note that the stellar evolution parameters may be tweaked to produce a small amount of normal Type Ib/c supernovae. Obtaining a reliable metallicity dependence of these ratios should easily distinguish these progenitors. But be aware that stellar evolution remains a field involving many free parameters. Although Heger et al. (2003) make some solid claims to compare against observations, new features, such as the mixing models of Yoon & Langer (2005), can easily change these predictions. The predictions of binary models are, perhaps surprisingly, a little more solid. But since they too depend on stellar models, we must interpret any of these predictions with caution as well.

Table 1 shows the differences between single- and binary-

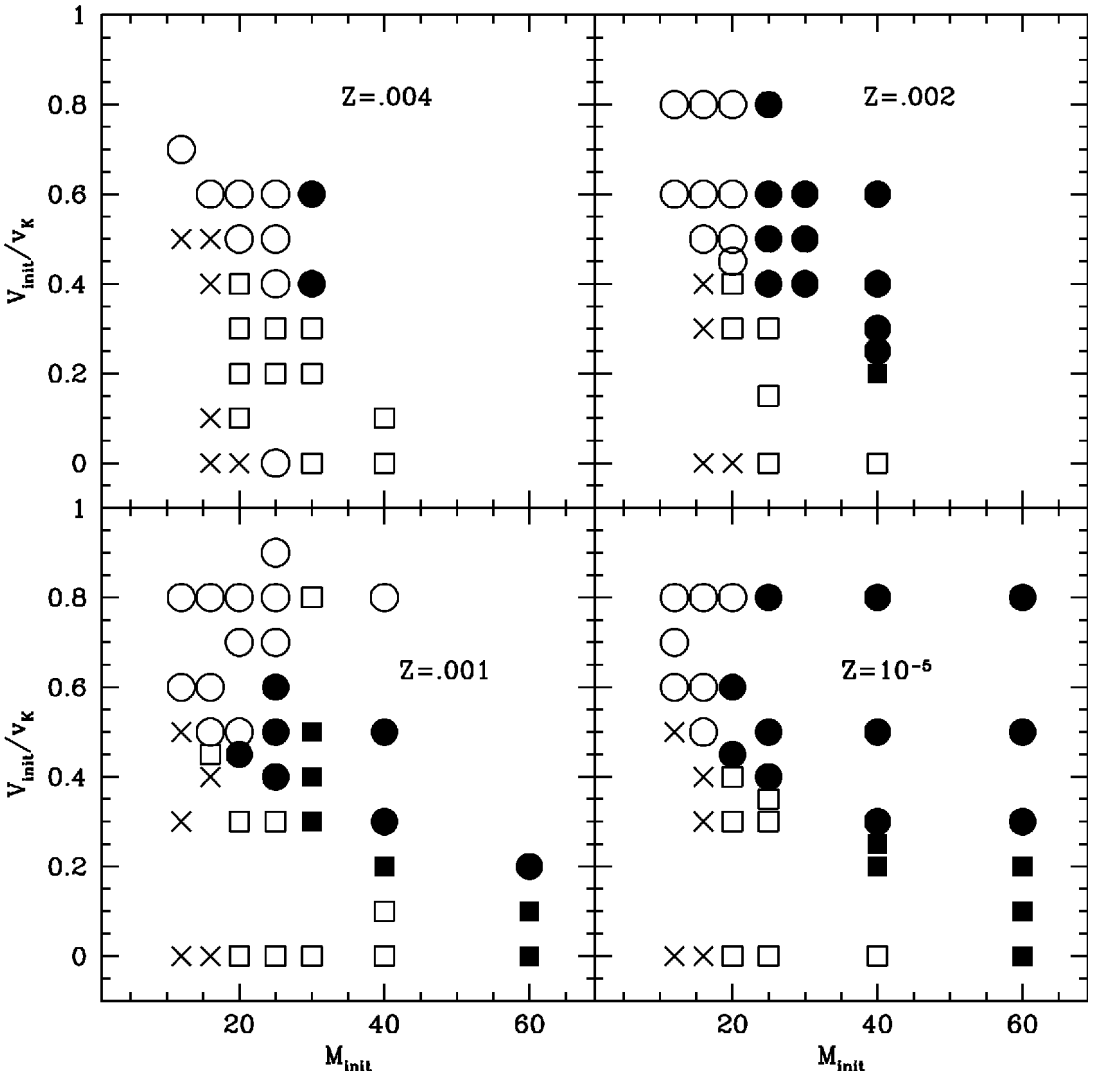

FIG. 6.—Fate of massive single stars as a function of initial mass and spin period. The squares correspond to Type II (H-rich) collapses, and the circles correspond to Type Ib/c (H-deficient) collapses. Filled symbols correspond to direct collapse objects, open symbols correspond to weak SN explosions, and the crosses correspond to normal SN explosions. There are no normal Ib/c SNe produced with this particular grid of stars from Yoon et al. (2006). These stellar models ended at core C/O burning, so we do not have a collapsed core to examine to determine its true fate. Instead, we use the C/O core mass, using the Fryer (1999) analysis and comparing the cores of those collapsing C/O cores to the C/O cores presented by Yoon et al. (2006). For normal stars, Fryer (1999) predicts that stars with low mass loss and initial masses above roughly 20 $M_{\odot}$ will produce weak SN explosions and black holes and stars above 45 $M_{\odot}$ do not produce SNe explosions at all (although both these types of objects may produce GRBs and their associated SNe). The size of the C/O core varies from simulation to simulation. The Limongi & Chieffi (2006) C/O cores tend to be 20% lower than their Woosley et al. (2002) counterparts. The Yoon et al. (2006) cores tend to be 30% smaller, but this is, in part, due to the fact that no post-C/O core ignition shell burning contributes to the C/O core mass. We chose a 4 $M_{\odot}$ C/O core mass for the dividing line between strong and weak SN explosions and a 13 $M_{\odot}$ dividing line between weak and no SN explosions, consistent with the Fryer (1999) analysis. Thirty percent variations in this mass limit will not vary the results significantly.

TABLE 1
TYPE IB/C SUPERNOVAE

Scenario	Normal Supernovae	Weak Supernovae[a]
Single	Rate $\downarrow Z \downarrow$, rate = 0 for $Z < Z_{\rm critical}$[b]	Weak Ib/c SNe dominate at $Z_{\odot}$
Binary	Rate $\downarrow Z \downarrow$, rate = 1%–10% solar rate for $Z < Z_{\rm critical}$[b]	Weak Ib/c SN trend follows strong Ib/c SNe
Observations	Rate $\downarrow Z \downarrow$	No data

[a] Stars that collapse with large cores are likely to produce weak supernovae whether or not the hydrogen envelope remains.
[b] The $Z_{\rm critical}$ could be at solar metallicity for single stars. It is likely to be at lower metallicities for binary stars (~0.5 solar).

TABLE 2
THEORETICAL PREDICTIONS: GRBs

Scenario	Angular Momentum	Metallicity Trend	Surrounding Environment	Associated Supernovae
Classic single	Low?	Rate peaks $\sim 0.1\ Z_\odot$	High wind	H-rich to He-rich
Mixing single	Good	$Z < 0.1\ Z_\odot$	Low wind	All He-rich
Classic binary	Low?	Rate $\uparrow$ $Z \downarrow$	Tends to low wind	He-rich, He-poor
Tidal binary	Good?	Rate $\uparrow$ $Z \downarrow$	Tends to low wind	He-rich, He-poor
Brown merger	Good?	Rate $\uparrow$ $Z \downarrow$	Tends to low wind	He-rich, He-poor
Explosive ejection	Good?	Rate $\uparrow$ $Z \downarrow$	Shell within 1 pc	He-poor
He merger	High	Rate $\uparrow$ $Z \downarrow$	Tends to low wind	He-rich, He-poor
He case C	Good?	Rate $\uparrow$ $Z \downarrow$	Tends to low wind	He-rich, more He-poor
Cluster	Good?	Rate $\uparrow$ $Z \downarrow$	Tends to low wind?	He-rich?

star progenitors for Type Ib/c supernovae. Unfortunately, uncertainties in stellar evolution prevent us from making firm predictions about anything.

2.2. Progenitors for Hypernovae

Most of our progenitors will focus on the collapsar engine with its three basic requirements: (1) the model must form a black hole in the center of a star, (2) the model must produce sufficient angular momentum in the star to form a disk around the black hole (but not too much angular momentum to limit the accretion rate), and (3) the model must eject the hydrogen envelope so that the jet produced by the collapsar engine can punch out of the star. We will broaden our scope to include any progenitor that produces a nondegenerate star accreting rapidly onto a compact remnant (either neutron star or black hole). For most of our progenitors, this opens up only a slightly broader range of systems with rapid fallback. It also includes such progenitors as the He-merger scenario in which a compact remnant spirals into the center of its stellar companion (Fryer & Woosley 1998). The list of all the progenitors studied and their basic predictions is given in Table 2. Before we discuss each progenitor individually, let us first discuss the generic trends that we expect from these three constraints.

Black Hole Formation.—Nearly every GRB progenitor currently proposed requires the collapse of a massive star down to a black hole (or a massive neutron star). This constraint is equivalent to restricting GRB progenitors to those stars that produce a weak or no explosion under the standard core-collapse supernova engine (see Fryer 2003 for a review). It is commonly assumed that the mass of the progenitor star determines whether it will produce a strong or weak supernova explosion. Although the exact mechanism behind core-collapse supernovae is not known, current studies have focused on the role of the convective engine between the surface of the neutron star and the accretion shock of the infalling atmosphere. If this convection region is indeed the critical aspect of core collapse determining the strength of the standard supernova explosion, a consistent picture can be developed describing the fate of a collapsing star as a function of its mass. Under this assumption, Fryer (1999) argued that, in the absence of stellar winds, the more massive stars ($\gtrsim 20\ M_\odot$) would fail to produce strong explosions and collapse to form black holes. His argument was based on two facts: (1) the ram pressure at the top of the convective region is larger for more massive stars, making it more difficult to explode these stars and leading to explosions that take longer to develop and are weaker and (2) the binding energy of stellar material increases dramatically with increasing star mass. Fryer argued that even though the uncertainties in the explosion engine were great, these two combined effects allowed fairly accurate precision in determining the transition between neutron star and black hole formation ($23 \pm 5\ M_\odot$).

The transition between neutron star and black hole formation at about the mass range has also been suggested empirically (using spectra and light curves; Nomoto et al. 2003, 2006a, 2006b). It may well be that explosions in this transition region (between 20 and $30\ M_\odot$) can teach us more about the supernova explosion mechanism than any other objects (Nomoto et al. 2006a). An obvious example is SN 2005bf, whose double-peaked light curve and unipolar feature in the spectra may well be an indication of a transition object (Maeda et al. 2007).

What Fryer (1999) had not considered were the uncertainties in stellar evolution. His results were entirely based on the Woosley & Weaver (1995) progenitors, which did not include the effects of mass loss from stellar winds or rotation. Fryer (2006) developed an analytic means to estimate the final mass of the compact remnant after a supernova explosion. The results for several nonrotating presupernova models are shown in Figure 7. The lines show the results of the Woosley et al. (2002) progenitor models (dotted line refers to solar metallicity; solid line refers to very low metallicity), and the points arise from the Limongi & Chieffi (2006) progenitor models for solar (*circles*), 0.2 solar (*squares*), and zero (*triangle*) metallicities. For solar metallicity, all massive stars produce weak explosions that then accrete through fallback (above $\sim 20\ M_\odot$, these stars form black holes).

At lower metallicities, some stars will collapse directly down to black holes, producing no explosion under the standard core-collapse engine. The original "collapsar" engine argued that GRBs are produced by stars that collapse directly down to black holes (Woosley 1993). If this is indeed a requirement, we find

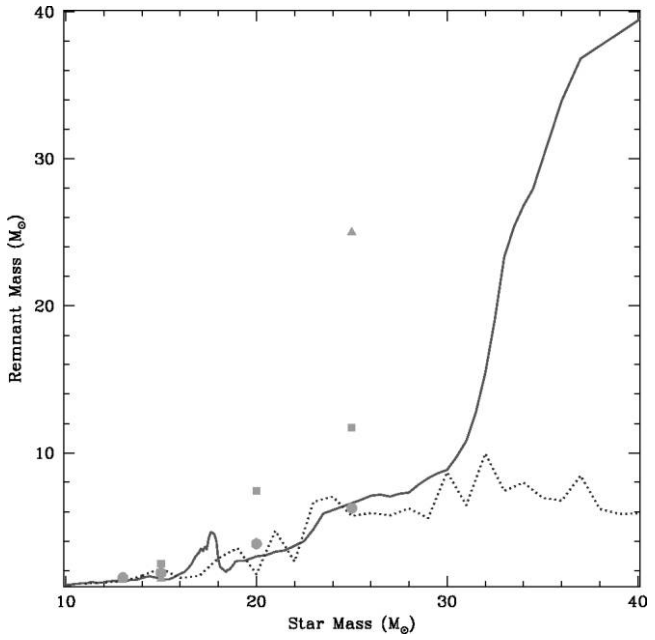

FIG. 7.—Remnant mass using the Fryer (2006) analysis vs. initial star mass for both the Limongi & Chieffi (2006) and the Woosley et al. (2002) stellar progenitors. The lines are derived from the Woosley et al. (2002) progenitors: dotted line refers to solar metallicity, solid line refers to very low metallicity. The points are derived from the Limongi & Chieffi (2006) models for solar (*circles*), 0.2 solar (*squares*), and zero (*triangle*) metallicities. Around 20 $M_\odot$, the fate of the stars depends sensitively on the stellar evolution code used. However, it is clear that around 20 $M_\odot$ is roughly the dividing line between neutron star and black hole formation. [*See the electronic edition of PASP for a color version of this figure.*]

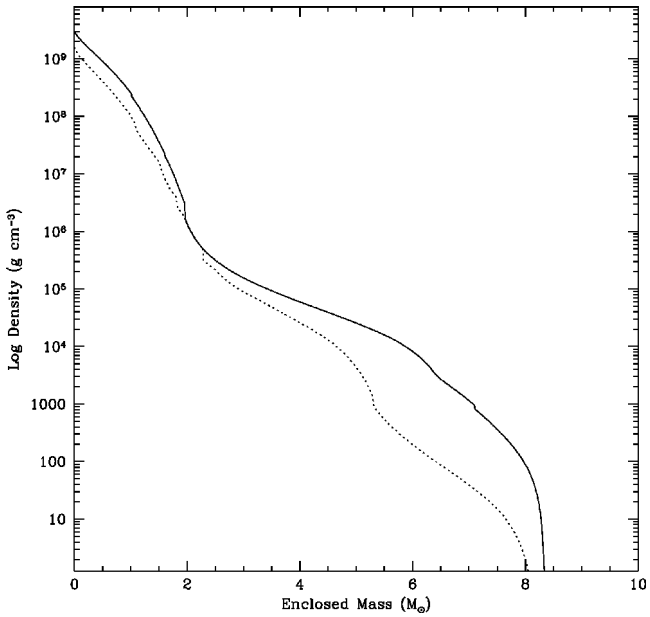

FIG. 8.—Density profiles of the Limongi & Chieffi (2006) and Woosley et al. (2002) 25 $M_\odot$ stars at collapse. The differences in the inner 1 $M_\odot$ can be explained by the fact that the models are at different stages in the collapse. A difference of a fraction of a second can cause the difference in densities in this inner region. But the differences beyond this inner core (beyond 2 $M_\odot$) can only be explained by uncertainties in the stellar evolution models.

from the Heger et al. (2003) progenitors that GRBs are not produced at solar metallicity. At low metallicity, stars above 30 $M_\odot$ form GRBs (Fig. 7, *solid line*). The Limongi & Chieffi (2006) progenitors show similar trends at solar metallicity (no direct collapse GRBs at solar metallicity) but exhibit quite different fates at zero metallicity. The 25 $M_\odot$ stars at zero metallicity will collapse directly to black holes.

Looking back at Figure 7, it is clear that above 20 $M_\odot$, the results of stellar evolution models vary drastically. Figure 8 shows the difference between the 25 $M_\odot$ stars produced by Woosley et al. (2002) and by Limongi & Chieffi (2006). These differences are believed to arise from different recipes for mass loss from stellar winds and for convective mixing. We discuss mass loss below when we discuss uncovering the hydrogen envelope. As for mixing, recent studies by Young et al. (2005) have shown that the structure of the stellar core can change drastically when different mixing-length algorithms are used. TYCHO, the stellar evolution code originally developed by Arnett, is being upgraded to incorporate more realistic mixing algorithms based on multidimensional simulations (Meakin & Arnett 2006), but thus far, the progenitors available are produced by codes using mixing-length convection.

Other effects might include the initial rotation of the star. Fryer & Heger (2000) found that extreme rotation dampened the convection along the rotational equator, ultimately leading to a weaker explosion. This 15 $M_\odot$ star ultimately had considerable fallback, forming a black hole (A. L. Hungerford et al. 2008, in preparation). Others have found that rotation can lead to asymmetric neutrino heating that helps to drive convection and ultimately a supernova explosion (Shimizu et al. 1994; Kotake et al. 2003). In addition, as we discuss below, Yoon & Langer (2005) found that rapid rotation could lead to extensive mixing that burns most of the hydrogen envelope into helium, producing larger and denser cores that are more likely to collapse directly to black holes. Both of these effects will lower the limiting mass for black hole formation (both through direct collapse and through fallback).

Let us summarize what we have learned. Because nearly all of the progenitors currently suggested require the formation of a black hole, all predict that it should be easier to form GRBs at lower metallicities where weaker winds allow more massive cores. If a progenitor requires the direct collapse of the star's core into a black hole (most of the currently proposed progenitors do not distinguish between fallback and direct-collapse black holes), current models suggest that GRBs will not occur at solar metallicity. These models also predict that if we are limited to direct-collapse black holes, only stars above ~25–40 $M_\odot$ (depending on the choice of stellar evolution code) will

produce GRBs. Last, the biggest uncertainty in such calculations lies in our poor understanding of stellar evolution, and it is unlikely that we will constrain GRB progenitors beyond this current state until real progress is made with these models.

Angular Momentum.—With respect to angular momentum, the progenitors for GRBs can be divided into two classes: those that are born rotating rapidly and retain enough of their birth angular momenta to produce a black hole accretion disk, and those that are spun up through interaction with another star (either tidal forces or merger events). Achieving sufficiently high angular momenta in the collapsing cores is potentially the strongest constraint on any progenitor. Unfortunately, stellar evolution models studying angular momentum are still primitive: they generally neglect centrifugal forces (which can be important for the high spin rates required to make GRBs), they incorporate recipes for the generation and angular momentum transport effects of magnetic fields that may or may not be accurate, and they depend sensitively on the loss of angular momentum through winds (Hirschi et al. 2005; Woosley & Heger 2006; Meynet & Maeder 2007). The current state of affairs is that stars with very fast initial spin periods may retain enough angular momentum to produce an accretion disk if the mass loss is sufficiently low.

For many binary progenitor models, the binary component is used to remove the hydrogen envelope without the angular momentum loss that occurs in wind mass loss. However, some binary models have been proposed that use the binary to inject angular momentum into the star at later stages in the star's evolution. The helium-merger model of Fryer & Woosley (1998) argues that a compact star (either neutron star or black hole) merges with its companion, injecting angular momentum as it spirals into the companion's core. This model definitely will add angular momentum, maybe even too much (Di Matteo et al. 2002; Fryer et al. 2006b).

Ejecting the Hydrogen Envelope.—The ejection of the hydrogen envelope can occur either through stellar winds or binary mass ejection. For single stars, where we must rely on stellar winds, this allows us to place constraints on the metallicity of progenitors. Heger et al. (2003) found that only a fraction of single stars will both remove their hydrogen envelopes and collapse to form black holes (they did not consider constraints to fit the rotation requirements). Figure 9 shows GRB rate as a function of metallicity using the results of Heger et al. (2003) assuming that all stars have sufficient angular momentum to form a disk. Note that the peak GRB rate occurs near 0.4 $Z_{\odot}$. The decrease above this metallicity value occurs because fewer and fewer stars collapse to form black holes. But the decrease below the peak metallicity value occurs because fewer and fewer stars lose their hydrogen envelopes.

As we see below, binary models avoid this constraint by definition: binary models all invoke a mass transfer phase that removes most or all of the hydrogen envelope. The Yoon & Langer single-star models also avoid this constraint. But there is a growing belief that GRBs lose their helium envelopes as well (the supernovae associated with GRBs do not exhibit strong helium lines). If so, the Yoon & Langer single-star model is ruled out. Without a better understanding of winds, we cannot say much more about this constraint other than the fact that it will be more restrictive for single-star models.

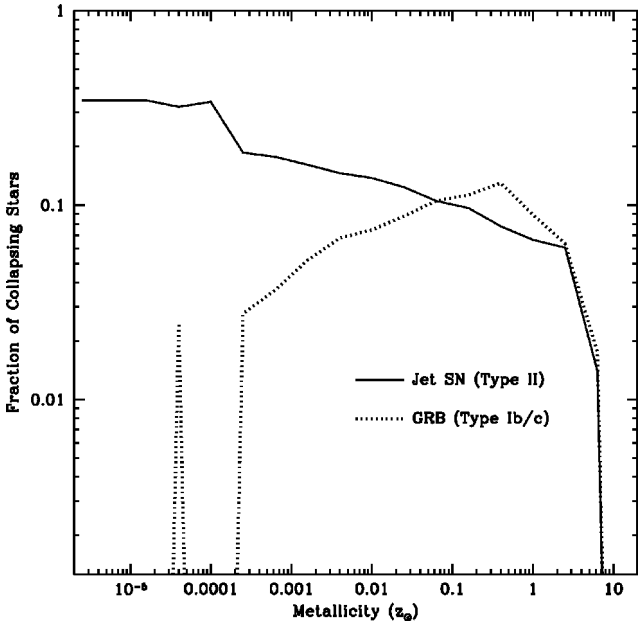

FIG. 9.—GRB rate as a function of collapsing stars for single stars as a function of metallicity using the Heger et al. (2003) models. The solid line shows those possible hypernovae with hydrogen envelopes (termed "jet" SNe by Heger et al. 2003). The dotted line shows systems that lose their hydrogen envelopes and hence *could* be GRB progenitors. These numbers must be multiplied by a factor indicating what fraction of these stars actually retain enough angular momentum to make black hole accretion disks (could be 0). To make single models work, we must somehow explain why we do not observe jet SNe (currently a matter of debate in stellar evolution theory).

2.2.1. Single-Star Models

Single-star models can be grouped into two types of progenitors: a single star with strong winds that eject the entire hydrogen envelope (Fryer et al. 1999) and a single star with extensive mixing that burns most of the hydrogen to helium (Yoon & Langer 2005; Woosley & Heger 2006). The high mass-loss case argues that the progenitors arise from a subset of Wolf-Rayet stars with enough mass at collapse to form black holes and enough angular momentum to form a disk. Unfortunately, most massive stars that lose their hydrogen envelopes also lose so much mass that they do not collapse to form black holes. Using the models of Heger et al. (2003), we find that the stars that both lose their hydrogen envelopes and still collapse to form a black hole lie within a narrow range of masses depending on metallicity: ~32–40 $M_{\odot}$ at twice solar metallicity, ~34–60 $M_{\odot}$ at solar metallicity, $\gtrsim$36 $M_{\odot}$ at roughly 1/10th solar metallicity, and $\gtrsim$60 $M_{\odot}$ at roughly 1/1000th solar me-

tallicity. The fraction of stars forming GRB progenitors peaks at metallicities around 1/10th solar for this progenitor scenario. However, single-star stellar evolution models including rotation have had trouble getting enough angular momentum in the core to produce GRBs (Woosley & Heger 2006). Winds can significantly reduce the angular momentum (Hirschi et al. 2005), making achieving the required angular momenta in the core very difficult for this progenitor. Indeed, we expect faster rotating cores in those stars that retain their hydrogen envelopes, predicting a larger population of hydrogen-rich hypernovae than the observed hydrogen-poor class. We term this progenitor the "classic single-star" scenario. The primary uncertainty in this calculation lies in the angular momentum transport present in the stellar evolution models.

An alternate single-star model has recently been proposed by Yoon & Langer (2005) and Woosley & Heger (2006), in which a rapidly rotating core can develop extensive mixing, burning nearly the entire hydrogen envelope into helium. Such a star becomes a helium star not by ejecting its hydrogen envelope but by burning the hydrogen into helium. This model will only work with fast-rotating cores at low metallicities (less than 1/10th solar). However, this constraint is actually a constraint on the mass-loss rate, and it may be that the maximum metallicity that can be accommodated is higher. High core rotation rates can be attained for these stars, and the large helium core masses lead to larger cores, which are more likely to collapse to black holes. This model predicts no GRBs to be produced at metallicities above 1/10th solar. The low metallicities also argue for weak winds. We do not expect any hydrogen-rich hypernovae or many helium-poor hypernovae from this progenitor. We term this the "mixing single-star" scenario.

2.2.2. Binary Mass Transfer Models

One way to avoid the problem of loss of angular momentum in a stellar wind is to eject the hydrogen envelope via binary mass transfer (Fryer et al. 1999). An example of such a progenitor is a binary system where, when the more massive star evolves off the main sequence, it expands and envelops its companion. The companion then spirals in toward the core of the massive star, ultimately ejecting the envelope of the massive star (turning it into a helium star) and producing a close binary system. In this simple case, the effect of the binary is only to eject the hydrogen envelope. The fraction of these systems that form hypernovae depends on the fraction of stars that are in close binaries (presumably lower at low metallicity because low-metallicity stars do not expand as much),[22] the fraction of stars that collapse to form black holes (larger at low metallicity), and the angular momentum evolution of massive stars. It is likely that the fraction goes up with decreasing metallicity, but stellar evolution models are not at the level that they can answer these questions yet. Some bursts will have strong winds, but it is likely that more will have weak winds (strong winds will lead to the formation of neutron stars, not black holes). None of these progenitors will be hydrogen-rich, and some will be helium-poor. We term this model the "classic binary" scenario.

A subset of these systems will produce such tight binaries after the mass transfer phase that the two stars will become tidally locked (as suggested by Izzard et al. 2004; see also Tutukov & Cherepaschuck 2004). In this manner the binary would not only remove the hydrogen envelope but also spin up the massive star. If the angular momentum is conserved through the collapse, it may be more than sufficient to form a black hole accretion disk. To determine whether such a mechanism can work, two issues must be tested.

First, we must ensure that tidal synchronization is sufficiently fast for it to occur in our quickly evolving stars. Van den Heuvel & Yoon (2006, 2007) calculated these timescales for helium stars. They found that if the inspiral companion of the helium star is a Roche lobe–filling solar-type main-sequence star (typical orbits around 6–8 hr), the helium star reaches tidal synchronization in a fraction of its lifetime. The core of the helium star, during its contraction toward C-burning and later stages, increases its rotation rate but, because of the magnetic coupling between core and envelope (using the Spruit [2002] mechanism), is slowed down so much that at the time of core collapse it has insufficient angular momentum to produce a GRB.

On the other hand, van den Heuvel and Yoon found that if the companion of the helium star is itself a compact object, the shortest possible orbital periods are ~1–2 hr, and in this case, with the same prescription the core has sufficient angular momentum to make a GRB. Their results therefore suggest that only compact binary systems that descended from high-mass X-ray binaries (HMXBs) would be able to produce GRBs. They argue that several well-known Galactic HMXBs, such as Cyg X-1 and 4U 1223−62, are excellent prospective progenitors of these very close helium-star–plus–compact-star binaries and that systems of this type may be produced in sufficiently large numbers to make a sizeable contribution to the long-duration GRB formation rate. The preference of long-duration GRBs for small, lower metallicity, star-forming galaxies (see below) would then be due to the lower wind mass-loss rates in low-metallicity massive stars (e.g., see Lamers & Casinelli 1999; Mokiem 2006), which favors black hole formation over neutron star formation at stellar collapse.

Belczynski et al. (2007) discovered this same result by studying a series of progenitors with and without this tidal locking effect. As a base model, they assumed no tidal locking and a standard progenitor with reasonably fast rotation at birth but included the mechanism by Spruit (2002) for magnetic braking. For their tidal calculations, they used this same base model, but for those stars for which the radius of the star was greater than $0.2a(1 - e)$, where a is the orbital separation and e is the eccentricity, they assumed that the star was completely synchronized. Although a population of the secondary stars are

[22] This trend is not completely accepted in the stellar community.

spun up (the previously mentioned HMXBs), the bulk of the close binaries are slowed down by tidal effects. Those that are spun up are quite rare and unlikely to match the observed GRB rate.

2.2.3. Binary Merger Models

If we include magnetic braking (using the Spruit [2002] mechanism) in stellar evolution models, we find that neither of the binary mass transfer models currently have core angular momenta at collapse that are sufficient to produce collapsars (Woosley & Heger 2006; however, see van den Heuvel & Yoon 2007 and above). This leads one to suggest increasingly exotic progenitors. One such progenitor argues that the two stars in the binary have nearly equal masses and hence the companion evolves off the main sequence before the more massive star collapses (so that the binary goes through two common-envelope phases prior to collapse). In the second common-envelope phase, the stars merge, producing a single massive star, which has lost most of the hydrogen envelopes of both stars (Fryer et al. 1999). The merger process injects much of the orbital angular momentum of the binary into the merged star, providing considerable spin-up with a nearly bare helium star. It is assumed that winds will remove the rest of the envelope. Simulations have shown that if neither star has begun helium burning before the merger, the final collapsed core will be spinning slightly faster than its single-star counterpart (Fryer & Heger 2005). It is likely that if the more massive star is well through helium burning, this spin-up will be more dramatic, but simulations to confirm this trend have yet to be done. This progenitor will have observational trends similar to those of the binary mass transfer scenarios. Initially named the helium-helium merger scenario by Fryer et al. (1998), this name has produced incredible confusion with the He-merger model below, so in this review, we rename it. In deference to the Bethe & Brown (1998) proposal to use equal-mass stellar binaries to make double neutron star binaries, we term this the "Brown merger" scenario.

An additional progenitor scenario based on the new route for common-envelope ejection was discovered by Ivanova and collaborators (Ivanova & Podsiadlowski 2003; Podsiadlowski et al. 2007). They noticed that in case C common-envelope phases, the inspiraling secondary star can actually overfill its Roche lobe and accrete onto the helium core of the primary. This accreting material will affect the core in two ways. First, this mass accretion will spin up the core. Second, the material streaming from the secondary can penetrate deep into the helium core and ignite, producing explosions that eject not only the helium shell but the hydrogen envelope as well (Ivanova & Podsiadlowski 2003). The final product of this explosive mass ejection is a pure CO core, consistent with current observations of the supernovae associated with GRBs. Since this scenario only occurs in case C mass transfer, the GRB will occur shortly after (within 10^4 yr) the explosive mass ejection and the shell from this common-envelope ejection should still be relatively close (within roughly 1 pc). We term this scenario the "explosive ejection" scenario.

2.2.4. He-*Merger Model*

Fryer & Woosley (1998) proposed a model akin to the bulk of the collapsar models arguing that the merger of a neutron star or black hole with its companion could produce a collapsarlike outburst. In this formation scenario, the binary first evolves into a neutron star or black hole binary (observed as X-ray binaries). In many conditions, the companion eventually envelops the compact object, causing it to spiral into the center of the companion star. This progenitor avoids the difficulties involved in forming black holes, and it easily spins up the collapsing star enough to form a disk. However, it may have too much angular momentum (Di Matteo et al. 2002; Fryer et al. 2006b). Compared to the mass transfer and single-star scenarios, it is not so strongly dependent on the metallicity. But since the binary is likely to be kicked in the formation of the compact remnant, the binary can move significantly beyond its formation site and may not be enshrouded in a stellar wind (it will, however, have a torus of ejected envelope material in the equator of the rotation axis and GRB jet). Very few of these progenitors will be hydrogen-rich, but one would expect the bulk of them to be helium-rich. This is the "He-merger" scenario.

One way to overcome the angular momentum problem is to assume that the common-envelope phase occurs after helium burning (case C mass transfer). In this case, the moment of inertia of the C/O core will be larger, and the inspiraling neutron star will have lost much of its orbital angular momentum, leading to slower rotation. If only these mergers lead to a collapsar engine, a large fraction may be helium-poor. Otherwise, the observational properties of this subclass of He mergers is similar to the classical He-merger scenario. We term this the "helium case C" scenario.

2.2.5. Cluster Models

Kulkarni has proposed that perhaps the progenitor requires interactions in a cluster. Two possibilities for such a progenitor include cluster enhanced mergers, currently invoked to form intermediate-mass black holes (Portegies-Zwart et al. 2005), or mergers between compact remnants and stars. These mergers may well produce massive, rapidly spinning cores. They also will be more common in low-metallicity systems. Thus far, no detailed studies have been done on these systems.

3. OBSERVATIONAL CONSTRAINTS

By 1992, the number of gamma-ray burst models proposed by theorists had grown to over 100 (Nemiroff 1994). Although many of these models stretched the limits of physics, the bulk were only discarded when it was shown that the models did not match observations (or did not match the observations as

TABLE 3
OBSERVATIONAL CONSTRAINTS: GRBS

Observation	Strong Constraint	Trend
Rate	$0.001 < R_{\rm GRB}/R_{\rm Ib/c} < 0.1$	$R_{\rm GRB} \approx 0.1 R_{\rm Ib/c}$
Associated SN	Some are Ic	All are Ic
Metallicity	Range: 0.01–1 solar	Mean ~1/2–1/3
Surrounding environment	None strong	Free-streaming wind limited to 1 pc
Weak supernovae	None strong	Fallback BHs must occur
Host morphology	None strong	Interacting galaxies (star formation/low metallicity?)
Distribution	$M_{\rm prog} \gtrsim 25\ M_\odot$	Possibility cluster effects important
Gravitational waves	None yet	Possibility to constrain angular momentum

well as other models). Rightly so, observations are used as the final arbiter in theoretical disputes and have played a major role in our understanding of GRB and SN progenitors. Here we discuss those observations that can be used to constrain GRB and Type Ib/c progenitors. For each constraint, we outline both the strong result (what we believe is robust) and the trend (what is implied by the data). These results are summarized in Table 3.

3.1. Rates

As theorists introduce increasingly exotic progenitors for GRBs, the rate of these bursts becomes an ideal constraint on the models. Any proposed model must be able to produce bursts at a rate comparable to the observed rate. Generally, the mode of operation is to make sure that, under optimistic conditions, the GRB rate is larger than the observed rate. The reference value for the observed rate of GRBs per average galaxy has been estimated from the BATSE monitoring as $R_{\rm obs} \sim 10^{-7}\ {\rm yr}^{-1}$ (e.g., Zhang & Mészáros 2004), of which $\frac{2}{3}$ are long-duration GRBs. However, GRBs are highly beamed and can be detected only if the observer is within the small jet opening angle. This implies that the intrinsic GRB rate is likely a factor 10–100 higher, $R_{\rm true} \sim 10^{-6}$ to $10^{-5}\ {\rm yr}^{-1}\ {\rm galaxy}^{-1}$ (Podsiadlowski et al. 2004; Guetta & Della Valle 2007). There is evidence that the rate rapidly increases with redshift and is 10–100 times higher already at redshift $z = 1$ (Firmani et al. 2004; Matsubayashi et al. 2005).

The number above applies to the average or "normal" GRBs seen at cosmological distances. On the other hand, the recent discovery of underluminous, relatively nearby X-ray flashes (XRFs) and GRBs suggests the existence of a population of events less luminous but possibly 10^2 times more frequent (Pian et al. 2006). If these events are considered, the local rate of GRBs may be as high as $\sim 10^{-4}\ {\rm yr}^{-1}\ {\rm galaxy}^{-1}$.

The rate of all core-collapse SNe in the local universe is $6 \times 10^{-3}\ {\rm yr}^{-1}\ {\rm galaxy}^{-1}$ ($H_0 = 70\ {\rm km\ s}^{-1}\ {\rm Mpc}^{-1}$). According to the latest published estimates, still based on photographic/visual SN searches, Type Ib/c account for 15% of all core-collapse SNe, i.e., $\sim 10^{-3}\ {\rm yr}^{-1}$ (Cappellaro et al. 1999), although preliminary analysis of modern CCD SN searches suggests that this number may need to be increased by a factor of ~2. Li et al. (2007) and J. Leaman et al. (2007, in preparation) predict a rate of 30% ± 11%. About 5%–10% of the observed SNe Ib/c, showing high expansion velocity and bright luminosity, are usually dubbed hypernovae (Podsiadlowski et al. 2004; Richardson et al. 2006).

It has been found that the rate of core collapse also rapidly increases with redshift (Dahlen et al. 2004; Cappellaro et al. 2005), closely tracking the star formation history. This is consistent with the notion that the progenitors of both GRBs and core-collapse SNe are massive stars. At the moment there is no information on a possible evolution with redshift of the specific SN Ib/c or hypernova rate.

Even allowing for the large uncertainties of current GRB statistics, it is safe to conclude that only a small fraction (~1%–10%) of SNe Ib/c can be associated with GRBs, a fraction that appears to coincide with that of hypernovae. This corresponds to roughly ~1% of all core-collapse supernovae being GRBs. Such estimates are corroborated by radio surveys of supernova remnants (Soderberg et al. 2004; Gal-Yam et al. 2006a).

Theory estimates that roughly 5%–40% of all core-collapse stars collapse to form black holes (Fryer & Kalogera 2001). The primary uncertainty in this fraction comes from uncertainties in the initial mass function of massive stars. If ~1% of all core-collapse stars produce GRBs, this means that it may be that 20% of all black hole–forming stars must form GRBs. If the number were indeed this high, many of the current progenitors would be ruled out. However, with the current uncertainties in the rates and the initial mass function, this value could be as low as 1%, well within the range of the progenitors proposed here. But as the data and the theory behind the progenitors become more firm, it is likely that rate estimates will be able to rule out certain models.

The relative rates of Type Ib/c and Type II supernovae and GRBs may also rule out some of the progenitors. Some of the binary and single-star models make very different predictions for the metallicity dependence, and to a lesser extent redshift dependence, of the Type Ib/c–to–Type II supernova ratio (compare the results shown in Figs. 1 and 2). Reliable ratio values, discussed further below, could well rule out many of the models.

3.2. Supernovae Associated with Gamma-Ray Bursts

Collapsing massive stars that lose their hydrogen envelope are compact stars. Although their explosion mechanism is very different from Type Ia supernovae, they have the same rapid light-curve evolution and absence of hydrogen lines seen in

Type Ia supernovae and therefore are classified as Type I supernovae. Initially, Type I supernovae were in one class, but as more Type I supernovae were discovered with spectral appearances very different from standard I supernovae, the new classifications of Type Ib, and later Ic, were introduced (Wheeler et al. 1987; Harkness et al. 1987; see Filippenko 1997 for a review). In particular, SNe Ib have strong He lines in their spectra. These He lines strongly suggest that the origin of such supernovae is massive stars that have lost their hydrogen envelopes (Shigeyama et al. 1990).[23] Helium lines are notoriously difficult to excite. In a classic paper, Lucy (1991) showed that the high He I levels responsible for the optical lines cannot be significantly populated by thermal mechanisms at the temperatures typical of SN atmospheres. The most efficient mechanism is nonthermal excitation/ionization by the fast particles produced by the diffusion of the gamma rays and the positrons emitted in the decay of ^{56}Ni into ^{56}Co and then into ^{56}Fe. Departure coefficients of the order of 10^4–10^6 can be easily attained. The more ^{56}Ni that is mixed out into the He layer, the easier it is for nonthermal processes to take place. Therefore, seeing strong He I lines means both that nonthermal excitation/ionization is strong and that the mass of He in the ejecta is rather large. Typically, massive stars develop He shells with masses above $\approx 1\ M_\odot$ (Woosley et al. 2002; Yoon et al. 2006). Likely progenitors of SNe Ib are therefore WR stars, which lose their hydrogen envelope via strong stellar winds. Without the new Yoon & Langer (2005) mixing model or binary stars, the stars that produce these Ib supernovae must be more massive than $34\ M_\odot$ at solar metallicity (Heger et al. 2003). This limit moves upward at lower metallicities.

A later addition to the SN zoo, SNe Ic are characterized by the absence of both H and He in their spectra, as well as by the weakness or absence of the Si and S lines that are more typical of SNe Ia (again see Filippenko 1997). The obvious progenitors for SNe Ic are then stars that have lost both the H and He envelopes. The preexplosion star may thus be an early-type WR star, such as a WC star. However, it is not clear that such extreme stripping can be achieved in a single-star configuration. Nomoto et al. (1995b) suggested that SNe Ib come from single stars while SNe Ic come from binary stars. A binary configuration helps to remove the envelope (Podsiadlowski et al. 1992), and it may also address the angular momentum problem (see above). Actually, observationally there are many more SNe Ic ($\sim\frac{2}{3}$) than SNe Ib. This is against intuition in the single-star case and may be a further argument in favor of a binary origin for SNe Ic.

Some claims have been made of the presence of He lines in SNe Ic. These are mostly based on the difficulty in identifying a strong absorption line that is present near 1 μm in the early-time spectra of SNe Ic. One possible identification of the line is in fact He I 10830 Å. A similar situation actually exists for SNe Ia. In this latter case, Mazzali & Lucy (1998) showed that there are alternative possibilities (e.g., Si II, Mg I) and that if a strong He I 10830 Å line is present, then a strong 2 μm line is also expected. Infrared data of SNe Ic (Taubenberger et al. 2006) show that this is not the case. Therefore, if there is any He in SNe Ic, it is not a lot.

Thus far, there are only four well-observed cases of SNe associated with GRBs or XRFs: SN 1998bw/GRB 980425, SN 2003dh/GRB 030329, SN 2003lw/GRB 031203, and SN 2006aj/XRF 060218. All these SNe are of Type Ic, and they also share a broad-lined spectrum, which is indicative of the ejection of material at very high velocities $\sim$50,000 km s^{-1} (Iwamoto et al. 1998; Mazzali et al. 2003, 2006; Deng et al. 2005; Pian et al. 2006). Other broad-lined SNe Ic without GRBs are known (e.g., SN 1997ef, SN 2002ap, etc.; see Nomoto 2005 for a review). Broad-lined SNe Ic account for $\sim$5%–10% of all SNe Ic, and GRB/SNe account for $\sim$20% of all broad-lined SNe Ic. In contrast, no broad-lined SNe Ib have been observed, let alone in conjunction with a GRB. These numbers are beyond what the relative rate of SNe Ib versus Ic would predict, and one may therefore wonder whether having a SN Ic is a prerequisite for (1) ejecting material at high velocities and (2) producing a GRB (which is probably the most extreme part of result 1 and/or an orientation-dependent property).

Thus, any progenitor scenario must produce a reasonable number of progenitor stars that, at collapse, lose not only their hydrogen envelopes but also most of their helium envelopes. If the current trend holds, the observations could require that all progenitor stars must lose most of their helium envelopes.

3.3. Metallicity

A generic characteristic of massive stars is that these objects drive significant stellar winds. During the main-sequence lifetime of an O star, the mass-loss rate is $\approx 10^{-7}$ to $10^{-6}\ M_\odot$ yr^{-1} for stars of roughly solar abundance. The mass-loss rate rises dramatically ($>10^{-6}$ to $10^{-5}\ M_\odot$ yr^{-1}) during the red giant phase and later stages of the star's life (e.g., the Wolf-Rayet phase). Because these winds are driven by the radiation pressure of UV photons on metals in the stellar atmosphere, the wind mass-loss rates are predicted to be very sensitive to stellar metallicity (e.g., Nugis & Lamers 2000; Kudritzki 2000; Vink & de Koter 2005). Eldridge & Vink (2006) found that this metallicity dependence on the winds will produce a strong metallicity dependence on the formation of neutron stars versus black holes. One of the easier (although still quite difficult) predictions that a progenitor model can make lies in the metallicity dependence.

Evidence is growing that Type Ib/c supernovae preferentially occur in high-metallicity systems (Prantzos & Boissier 2003; Prieto et al. 2007). However, such surveys are still number limited with many possible selection biases. The fraction of systems at low metallicity will place strong constraints on our binary models. These results are summarized in Table 1.

For the foreseeable future, we are unlikely to develop an observational technique that will permit a direct metallicity measurement of a GRB progenitor. Perhaps the only prospect

[23] It is important to note that it was originally argued that these supernovae might arise from white dwarf progenitors (e.g., Branch & Nomoto 1986).

is if a GRB were to occur very nearby and one inferred the stellar metallicity from the SN ejecta. In lieu of this approach, observers can infer the metallicity of gas near the GRB progenitor using a few complementary approaches: (1) absorption-line spectroscopy of GRB afterglows, (2) emission-line spectroscopy of H II regions within the GRB host galaxy, (3) the slightly less direct method of measuring the interstellar extinction in the host (as dust content is related to metallicity), and (4) the very indirect measurement using the host galaxy morphology: if the hosts are small SMC/LMC-like galaxies, they are likely to have lower metallicity (see below). The first approach is currently limited to high-redshift ($z > 2$) GRB events. At lower redshifts, measurements of hydrogen via the Lyα, λ1215 transition require UV spectra and therefore space-borne telescopes. In contrast, the second approach is generally restricted to low redshift ($z < 0.6$) such that key emission lines remain in the optical spectrum. As such, there is no GRB host galaxy where the two techniques have been compared.

By comparing the column densities of hydrogen versus a metal (e.g., O, S, Fe), one can derive the metal abundance of the interstellar medium (ISM) surrounding the GRB. The observations are restricted to gas-phase abundances, and one preferentially focuses on nonrefractory elements (e.g., O, S, Zn) to minimize the effects of depletion onto dust grains. The spectra of GRB afterglows reveal strong interstellar absorption lines and damped Lyα profiles (e.g., Barth et al. 2003; Vreeswijk et al. 2004; Chen et al. 2005). The H I column densities are easily derived from even low-resolution, moderate signal-to-noise ratio observations by fitting the damping wings of the Lyα transition (e.g., Jakobsson et al. 2006). An accurate determination of metal-line column densities, however, is challenged by the very large observed equivalent widths (e.g., Savaglio et al. 2003). First efforts reported metal column densities based on traditional single-component, curve-of-growth (COG) analysis (e.g., Savaglio et al. 2003), yet high-resolution observations of GRB afterglows indicate that the COG results systematically underestimate the metal abundance (Prochaska 2006). In general, one can estimate only a lower limit to the metallicity for spectra that do not resolve the line profiles.

Because the majority of observations to date were acquired with low-resolution spectrometers, there is a preponderance of lower limits to the metallicity (Prochaska 2006). In any case, the present set of metallicity measurements from $\approx$10 GRB afterglow spectra exhibit a large dispersion of values from $\approx$1/100 solar (Chen et al. 2005) to nearly solar metallicity (Castro et al. 2003). Many of the lower limits lie at $\approx$1/10 solar metallicity (Prochaska 2006), and, therefore, the mean (or median) value is at least this enriched. Furthermore, an average metallicity of $\frac{1}{3}$–$\frac{1}{2}$ solar is permitted if not suggested by the data. Even adopting the lower limits as values, the distribution currently lies along the upper threshold of damped Lyα metallicity measurements along quasar sight lines (Prochaska 2003). That is, the ISM measurements for GRB host galaxies match, and likely exceed, the cosmological mean metallicity in neutral gas at $z > 2$. In this respect, at least, the GRBs have average or even supersolar values. The full distribution of GRB metallicities from afterglow spectroscopy awaits the compilation of a much larger sample of echelle observations.

Apart from studying absorption and emission lines, one also can obtain information on the metallicity by measuring the interstellar extinction by dust in the host galaxy. Here all investigations find remarkably low dust contents in GRB hosts, the simplest interpretation of which is low metallicity. The interstellar extinction curves are very different from that of our galaxy. None of the hosts shows the 2175 Å extinction bump. The extinction curves of the hosts resemble more that of the SMC, which has a much higher gas-to-dust ratio than our galaxy. An important recent investigation by Starling et al. (2007) finds that, in all cases where the gas-to-dust ratio of hosts can be determined, it is equal to or larger than that of the SMC.

Before concluding our discussion of ISM metallicities, we wish to comment on two easily overlooked aspects of the measurements: (1) the relation of the observed gas to the GRB progenitor and (2) the abundance of Fe. Although one may expect the GRB progenitor to reside within a molecular cloud and/or to be surrounded by circumstellar material, afterglow spectra have not revealed strong evidence for this gas (Prochaska et al. 2006; Chen et al.2007). Furthermore, the GRB afterglow spectra almost always show strong Mg I absorption, which must occur at a distance >50 pc from the afterglow to avoid photoionization (Prochaska et al. 2006). Similarly, Vreeswijk et al. (2007) infer a distance to the ISM of $\approx$1 kpc based on their analysis of varying Fe^+ and Ni^+ fine-structure levels. These observations, therefore, indicate that the majority of neutral gas along the GRB sight line is at 100 pc to 1 kpc distance. In turn, the metallicity measurements must be considered at best a crude estimate for the GRB progenitor. The second point to emphasize is that the absorption-line measurements do not give a precise measurement of Fe or any other element on the Fe peak. This is due to their refractory nature; these elements are easily depleted from the gas phase onto dust grains. One can set a lower limit to the Fe-peak abundances from gas-phase measurements, but the corrections for differential depletion can exceed 1 order of magnitude. The metallicity values described above correspond solely to S, Si, and Zn, none of which dominate the opacity in massive stellar atmospheres. As it is reasonable to assume that the gas has an abundance pattern typical of massive star nucleosynthesis (i.e., α-enriched), the Fe abundance is likely $\approx$2 times lower than that recorded for Si or S.

Turning to lower redshift, one can infer the metallicity of the GRB progenitor by analyzing forbidden emission lines from H II regions within the host galaxy. Aside from very local galaxies, the observations generally contain emission from the entire galaxy. Nevertheless, one does not tend to observe very large metallicity gradients in H II regions (Kobulnicky 2005), and the derived value should correspond (within a factor of 2) to the local H II region. The analysis involves standard techniques of comparing line fluxes of forbidden H, O, and N transitions

against models of H II regions. To date, the results (which have been limited to GRB host galaxies at $z < 0.5$) reveal values of ≈1/10 solar metallicity (Prochaska et al. 2004; Sollerman et al. 2005). Stanek et al. (2006) have used these measurements to argue that low-z GRB host galaxies are biased to low metallicity under the assumption that GRBs trace current star formation. That is, a random sample of star-forming galaxies (weighted by current SFR) in the local universe would have higher average metallicity than that observed for the GRB host galaxies. At present, the small sample size precludes a strong conclusion regarding metallicity, but the results are suggestive of a selection bias. We also caution that the $z < 0.5$ GRB events have systematically lower energy than $z > 1$ events and one should not generalize these results to cosmological bursts.

Not surprisingly, the low-z GRB host galaxies also have low luminosity. Furthermore, Kewley et al. (2007) note that the GRB host galaxies also fall off the luminosity-metallicity (*L*-*Z*) trend observed for other low-z, irregular galaxies. The offset is in the sense that GRB host galaxies are either especially luminous for their metallicity or metal-poor given their luminosity. Given that GRBs are associated with short-lived massive stars, a possible explanation for the offset is that the star formation leads metal enrichment. That is, the galaxy is exhibiting a burst of star formation yet has not had sufficient time to enrich its H II regions. This is consistent with the observation that GRB host galaxies at $z \sim 1$ have very high specific star formation rates (SFR normalized to the galaxy luminosity; Christensen et al. 2004).

Finally, indirect evidence concerning the metallicities of long GRB environments may come from the study of the morphology of their host galaxies. Already several years ago it was noticed that the long GRB hosts tend to be small galaxies that are systematically bluer than the same size galaxies in the general population at similar redshifts. This suggests that they contain many massive stars and have a larger SFR than the general population of galaxies of similar size. Still, only a few GRB hosts show evidence of strong starbursts. It is not clear therefore that GRBs can be used to directly trace current SFR. A systematic, comparative study by Fruchter et al. (2006) compares 42 GRB host galaxies observed with the *Hubble Space Telescope* (*HST*) against the host galaxies of serendipitously *HST*-discovered core-collapse supernovae (CC-SNe; Types Ib/c and II) at the same general redshift ($z < 1.2$). This comparison shows striking differences between the two host galaxy populations and between the localizations of the explosions relative to the galaxies' light distributions. Specifically, of the 42 long GRB hosts, 41 appear to be small star-forming galaxies; only one of them is a grand design spiral, whereas half of the hosts of the CC-SNe at similar redshifts are grand design spirals. In addition, the locations of the GRBs on their host galaxies appear to be strongly concentrated on the optically brightest parts of their hosts, whereas the CC-SNe follow the average light distribution of their hosts. The bright spots on the light distribution of the GRB hosts are typically large concentrations of massive young stars (starbursts), similar to those observed in nearby blue dwarf galaxies such as NGC 3125, a galaxy with metallicity similar to that of the LMC/SMC (Hadfield & Crowther 2006), with a blue clump containing on the order of 10,000 O and Wolf-Rayet stars. Since the sizes of the GRB hosts are typically like those of the LMC and SMC, which have metallicities 0.3 and 0.2 solar, respectively, the morphology of the GRB hosts and the localizations of the GRBs on their hosts are therefore consistent with the idea that long GRBs occur at lower metallicities than their normal supernova counterparts. The work of Modjaz et al. (2007) corroborates these results. All of the progenitors listed in this paper require lower metallicities than normal supernovae. But what we mean by lower metallicity is still a subject of debate. Wolf & Podsiadlowski (2007) use the Fruchter et al. (2006) GRB host galaxy sample and show statistically that the median GRB host galaxy is a galaxy with the mass of the LMC and a metallicity of one-half solar. Indeed, they even argue that any model that requires a metallicity well below one-half solar can effectively be ruled out.

As to the normal CC-SNe: due to the shape of the IMF, one expects some 75% of all CC-SNe to originate from stars in the mass range 8–20 $M_{\odot}$, where core collapse produces neutron stars. The bulk of the CC-SNe are therefore expected to be neutron star–forming events. The striking difference between the morphologies of the long GRB hosts and the CC-SN hosts, as well as their differences in localization with respect to host light distribution, therefore strongly suggests that long GRBs are different from neutron star–forming supernovae. As pointed out by Fruchter et al. (2006), this is consistent with the picture that we are dealing here only with collapses of the cores of the most massive stars, which collapse to a black hole (or possibly other phenomena related only to the most massive stars).

At this point in time, it appears that there is no consistent picture of the metallicities of GRBs. We note however that direct measurements argue for higher metallicities, whereas the indirect measurements suggest lower metallicities.

3.4. Surrounding Environment

Some relevant properties of the medium around GRB progenitors can be extracted (at least, in principle) from observations of GRB afterglows in two ways. The more direct way is provided by understanding the origin of the absorption features seen in the afterglow optical spectrum. The less direct way is to compare the observed afterglow light curve with the analytical expectations for the blast-wave model, with the aim of constraining only the most generic properties of the burst ambient medium.

High-velocity absorption lines in afterglow spectrum.— High-velocity absorption lines of C IV and Si IV, blueshifted by 450, 1000, and 3100 km s^{-1}, have been identified in the optical spectrum of the GRB afterglow 021004 (Mirabel et al. 2002; Schaefer et al. 2003). C IV and lower ionization species' (Fe II, Al II, Mg II) absorption lines have also been seen in the

spectrum of GRB afterglow 020813 (Barth et al. 2003), at an outflowing velocity of 4300 km s^{-1}, and in that of GRB afterglow 030226, blueshifted by 2300 km s^{-1}. These velocities are too high to arise in a galaxy cluster; i.e., the absorbers must be in the GRB host galaxy. It cannot be ruled out definitely that the absorbers are the outflow of a now-dormant QSO or a superwind from a starburst region, but these origins are unlikely, given the required GRB direction–QSO outflow chance alignment and the lower velocity measured for starburst winds. If we can show that the lines must arise from the progenitor itself, we have a potentially strong constraint on the mass loss and collapse mass of the progenitor (e.g., van Marle et al. 2005).

Circumburst medium constraints from afterglow light curves.—The afterglow emission is believed to arise from the medium within 1 pc of the burst, which is energized by the relativistic shock driven by the GRB ejecta. The mechanism that generates magnetic fields of the order of 1 G in the shocked gas and accelerates electrons to at least 100 GeV (in the comoving frame) is not well understood, but such conditions must be met by the blast wave to radiate synchrotron emission at X-ray energies for days after the burst.

The decay of the afterglow light curve is determined by the dynamics of the forward shock, which energizes the burst ambient medium. Shortly after the burst, the blast wave becomes quasi-adiabatic (i.e., radiative losses are negligible), and, if there is no energy injection into the forward shock, the shock dynamics is determined only by the radial structure of the ambient medium and the collimation of the GRB outflow. Before collimation starts to affect the afterglow dynamics, the radius of the blast wave is $R_a(t) = 0.25(E_{s2}/n_0)^{1/4}[t_d/(z+1)]^{1/4}$ pc, where E_{s2} is the shock's kinetic energy per solid angle in units of 10^{52} ergs sr^{-1} (i.e., of the order of the GRB output), n_0 is the proton density at the location of the blast wave, and t_d is the observer time measured in days.

Therefore, the forward shock is within 1 pc of the GRB progenitor for the entire duration of the afterglow observations. The free winds of WR stars extend over 10 pc (Castor et al. 1975; Garcia-Segura et al. 1996); thus, the GRB ejecta should interact with the WR free wind. Then one expects that the afterglow light curve "reflects" its r^{-2} radial stratification. This simple test appears straightforward given that the afterglow model (e.g., Mészáros & Rees 1997) predicts a simple linear relationship between the exponent α of the afterglow light-curve power-law decay [$F(t) \propto t^{-\alpha}$] and the exponent β of the afterglow power-law spectrum ($F_\nu \propto \nu^{-\beta}$): $\alpha = 1.5\beta + c$, the stratification of the circumburst medium, $d \log n/d \log r$, setting the coefficient c.

There are two complications with the above test for the circumburst medium stratification. First, the coefficients of the relationship between α and β change if there is energy injection into the blast-wave energy and if the microphysical parameters that quantify the postshock energy in magnetic field and relativistic electrons evolve, which can hide the signature of the circumburst medium in the α-β relation. The X-ray light curves of *Swift* afterglows indicate that there may be a sustained energy injection in the blast wave for hours after the burst (Nousek et al. 2006; Panaitescu et al. 2006; Zhang et al. 2006). The second complication is that, at observing frequencies above the cooling frequency (ν_c), the afterglow emission arises from the medium that was swept up by the blast wave within less than one dynamical timescale, leading to a light-curve decay index α_X that is independent of the medium stratification. It is quite likely that the X-ray domain lies above ν_c; thus, the decay of X-ray light curves cannot constrain the circumburst medium stratification, as illustrated in Figure 8 of De Pasquale et al. (2006). The optical domain is more likely to be below ν_c, but a good determination of the optical spectral index β_o requires accurate near-IR measurements in order to have a sufficiently wide frequency baseline and to correct β_o for dust reddening in the host galaxy.

For a sample of two dozen pre-*Swift* GRB afterglows with optical decay indices and spectral slopes measured at about 1 day, the above α-β test identifies three cases that require a windlike medium and five for which the medium should be homogeneous; for the rest, the uncertainties of α and β are sufficiently large that either type of medium is allowed.

Another estimator of the ambient medium stratification results from comparing the optical and X-ray decay indices, α_o and α_X. If the cooling frequency ν_c is not between optical and X-ray, then $\alpha_o = \alpha_X$ and no information can be obtained in this way about the medium stratification. If ν_c is in between optical and X-ray, then $\alpha_o < \alpha_X$ for a homogeneous medium and $\alpha_o > \alpha_X$ for a wind. The different decay indices are caused by the evolution of ν_c: it decreases for a homogeneous medium and increases for a wind. This test is more robust because it relies only on light-curve decay indices, which can be measured more accurately than spectral slopes, and because energy injection in the blast wave speeds up the evolution of ν_c, which increases the difference between the optical and X-ray decay indices; i.e., the test is not "spoiled," a potential departure from the standard forward-shock model.

There are nearly three dozen GRB afterglows with measured decay indices α_o and α_X within the first day after trigger; only four of them exhibit the $\alpha_o > \alpha_X$ expected for a wind medium, while for 10 afterglows $\alpha_o < \alpha_X$ indicate a homogeneous medium; the rest provide an inconclusive test for the ambient medium.

A third method of assessing the structure of the burst ambient medium using afterglow observations applies to those afterglows whose power-law decaying light curves exhibit a steepening. Such a steepening is observed in the optical emission of pre-*Swift* afterglows at about 1 day and is most likely due to the collimation of the GRB ejecta, a light-curve break resulting when the blast wave has decelerated enough that the emission from the jet boundary becomes visible. A tight collimation of the GRB outflow, into a jet of half-opening angle less than 10°, is also desirable on energetic grounds, as the isotropic equivalent of many GRBs exceeds 10^{53} ergs, the out-

put of some bursts being even higher than 10^{53} ergs. However, we note that the X-ray emission of *Swift* afterglows (which have been followed less systematically in the optical) rarely exhibits a ~1 day break consistent with a jet origin (Willingale et al. 2006; Sato et al. 2007).

The existence of a jet break in the afterglow light curve allows us to distinguish between a homogeneous and a windlike medium through the fact that the slightly faster deceleration produced by the former leads to a shorter time during which the jet edge becomes visible and to a lower lateral spreading of the jet during this transition phase. The effect is a sharper light-curve break for a homogeneous medium than for a wind (Kumar & Panaitescu 2000). This is true also for a light-curve break resulting when the symmetry axis (of maximal ejecta kinetic energy per solid angle) of an angularly nonuniform outflow becomes visible to the observer (Panaitescu & Kumar 2003). Numerical calculations of the jet dynamics and its synchrotron emission are required to compare the shape of the light-curve break produced by a jet (or a structured outflow) and observations.

Table 4 lists the reduced χ^2 obtained for nine pre-*Swift* afterglows whose optical light curves exhibited a break. These afterglows have been monitored also at radio and X-ray frequencies, a multiwavelength afterglow coverage being necessary to constrain the blast-wave dynamical parameters that determine the jet Lorentz factor and lateral spreading during the light-curve steepening. Most of the best fits to the afterglows of Table 4 are not statistically acceptable; often, the large χ^2 is due to small-scale variations in the afterglow light curve, which the model cannot reproduce. In general, systematic differences between model and observed light curves are seen only for $\chi^2 > 4$. As can be seen from Table 4, only one afterglow is fit better with a windlike medium, while six are accommodated better by a homogeneous medium. The score is basically the same for the structured outflow model.

The conclusion that can be drawn from the above is that both the analytical and the numerical analyses of afterglow light curves indicate that the medium into which the GRB ejecta runs has a uniform density within the first parsec. A windlike medium, as expected around WR stars up to 10 pc, is sometimes compatible with the afterglow emission but does not seem to be the norm. Table 4 also shows that the uniform density inferred for those afterglows with a good multiwavelength coverage is in the 0.05–10 cm^{-3} range, which is close to the particle density expected for a WR wind at 0.1–1 pc. Thus, both the uniformity of burst ambient medium and the density that we obtain indicate that the region where the 0.1–10 day afterglow emission is produced is the shocked WR wind (e.g., Wijers 2001). It remains to understand why the extent of the freely expanding wind is so much smaller than expected.

The extent of the freely streaming wind arising from the GRB progenitor can be reduced from the extent predicted from our standard model either by decreasing the strength of the wind, increasing the density of the surrounding medium, or even increasing the pressure of the surrounding medium (Chevalier et al. 2004; van Marle et al. 2005; Fryer et al. 2006b). Higher densities and pressures in the surrounding medium are more likely in regions of high-mass star formation, also suggesting that the progenitors of GRBs are in the high-mass end of collapsing stars. Densities high enough to make a sufficiently small wind bubble are generally higher than those allowed by radio observations. Winds must be weakened substantially to make such a small wind bubble. Alternatively, removing the star from its original wind bubble as happens in some merger models can produce appropriate conditions. Wolf-Rayet mass-loss rates depend sensitively on the metallicity, and our above analyses assumed Wolf-Rayet mass-loss rates comparable to what one would expect for solar metallicity stars. To induce black hole formation, the GRB progenitor scenarios in this review all predict that most GRBs are produced at low metallicities. Single-star models require modest winds to eject their envelopes, but the winds of binary progenitors can be very weak. The helium merger progenitor can produce even weaker winds.

TABLE 4
REDUCED χ^2 OF THE BEST FITS OBTAINED FOR NINE GRB AFTERGLOWS

	Jet + n = const		Jet + Wind		SO + n = const		SO + Wind	
GRB	χ^2_ν	n (cm^{-3})	χ^2_ν	A_*	χ^2_ν	n (cm^{-3})	χ^2_ν	A_*
980519	2.6	0.1	1.8	2.0	2.4	4	1.4	0.6
990123	2.0	0.8	2.3	0.2	1.8	1	2.2	0.1
990510	0.78	0.3	3.1	0.4	2.1	2	4.6	0.8
991216	2.0	0.04	1.8	0.2	1.2	0.7	1.2	0.4
000301c	4.4	0.1	8.3	0.2	3.3	0.2	7.1	0.6
000926	2.2	20	3.5	1.8	2.2	3	2.8	0.5
010222	2.2	0.1	3.9	0.1	1.7	0.1	4.0	5
011211	4.7	1	8.7	0.6	2.3	1	4.7	0.7
020813	1.6	0.07	2.6	0.2	1.1	0.06	2.6	0.06

NOTE.—Reduced χ^2 of the best fits obtained for nine GRB afterglows (displaying optical light-curve breaks) with the jet model (uniform outflow with sharp boundaries) and SO model (structured outflow with a power-law angular distribution of ejecta kinetic energy per solid angle), for a homogeneous medium (best-fit density n is uncertain by a factor of 10) and a wind (density parameter A_* uncertain by a factor 2–3) (Panaitescu 2005).

It is difficult to place strong constraints at this time from observations of the surrounding medium. The simple models used to determine these quantities have many deficiencies, so it is difficult to be sure what the observations are truly telling us. However, the trend indicates that an ideal progenitor scenario will tend to produce wind ejecta that are limited to the inner 1 pc around the progenitor star. Further observations are required to provide a complete picture on this observational constraint.

3.5. Weak Supernovae Associated with GRBs

The cospatial and concurrent observation of supernovae associated with gamma-ray bursts provided the first convincing evidence that GRBs are produced in the collapse of massive

stars and propelled the collapsar model to the limelight as the leading model for GRBs. The luminosity of the supernova is roughly proportional to the total amount of ^{56}Ni produced in the explosion. Recent observations of two possible long-duration GRBs, produced in relatively typical star-forming galaxies, have no observed supernova associated with the GRB (Gehrels et al. 2006; Fynbo et al. 2006; Della Valle et al. 2006; Gal-Yam et al. 2006b; Ofek et al. 2007). It is possible that at least one, if not both, of these bursts are short bursts and, hence, not a constraint on a large-duration burst progenitors.

However, if these bursts are long-duration bursts, they can teach us a lot about collapsar progenitors. These weak associated supernovae were predicted by theorists (Nomoto et al. 2006a, 2006b; Fryer et al. 2006a), and light curves have now been calculated for these supernovae (Fryer et al. 2007). Observations of these supernovae have implications both for the mechanism through which the black holes of GRBs are formed and the site of nucleosynthesis for heavy elements such as ^{56}Ni in GRBs. If the bursts were indeed long-duration bursts, the observations imply that some GRBs produce very little ($\lesssim 0.07\ M_\odot$) ^{56}Ni. If this is true, this observation argues for some GRBs to arise from systems whose black hole forms via fallback, strongly constraining current models. But proving that these are long-duration bursts is far from given.

3.6. Host Galaxy Morphology

The morphological appearance of GRB host galaxies, particularly when compared to the general population of star-forming galaxies (for example in the HDF), may shed light on the environments and processes that are conducive to the formation of GRB progenitors. *Hubble Space Telescope* observations are available for about 50 GRB hosts, and recent visual and automated classification of these hosts led to several key results (Conselice et al. 2005; Wainwright et al. 2007). First, we find that the radial light distribution of most GRB hosts is exponential, as expected for disk galaxies (the median Sérsic index is about 1.1; Wainwright et al. 2007). Second, the median effective radius of the hosts is about 1.7 kpc, with a range of about 0.5–5 kpc. Third, GRB host galaxies follow the size-luminosity trend observed in other galaxy samples. However, thanks to the relative faintness of GRB hosts and the ability to measure their redshifts independent of the galaxy brightness, the GRB host sample extends the high-redshift size-luminosity relation by about 3 mag (Wainwright et al. 2007).

Most importantly, however, the overall morphological structure of the host galaxies indicates an overabundance of mergers/interactions compared to star-forming galaxies in the HDF. Overall, we find that about $\frac{2}{3}$ of all GRB host galaxies are morphologically disturbed. In the HDF, a similar fraction of galaxies appear to have an irregular morphology, but only at $z > 1$; at $z < 1$, about $\frac{3}{4}$ of all star-forming galaxies have a regular morphology (Wainwright et al. 2007). In addition, the proportion of interacting galaxies in the field increases with galaxy brightness (Conselice et al. 2003). The fact that the fraction of merging/interacting galaxies in the GRB sample is independent of both redshift and galaxy brightness indicates that these are regions of elevated star formation conducive to the formation of GRB progenitors. As a corollary, it appears that GRBs are less likely to occur in stable disk galaxies, and as a result GRB hosts at low redshift are more likely to present a biased population than at $z > 1$.

3.7. Distribution of Bursts with Respect to Intensity

The distribution of GRBs with respect to the light in a galaxy can also place constraints on the progenitor. Fruchter et al. (2006) found that, whereas normal supernovae traced the light in a galaxy, GRBs are actually more peaked toward the brightest regions in a galaxy. One of the more straightforward interpretations of this observation is that GRBs arise from a more massive population of stars than supernovae since the most massive stars are the most clustered (see also our discussion in the last part of § 3.3). It may also imply that there is some feature of clustering that is required to produce GRBs. Exactly what this result teaches us awaits a much more statistically significant set of observational data.

The strong constraint from this observation is that the progenitor system should arise from the most massive stars. If true clustering can be proved, this might lead to new progenitor models.

3.8. Related Stellar Systems

We may learn a lot about the progenitors of Type Ib/c SNe and GRBs from related star systems. For example, Smith et al. (2004) find a population of luminous blue variables (LBVs) at low luminosity [down to $\log(L/L_\odot) \sim 5.4$]. This is significantly lower than would be expected for the formation of LBVs through normal mechanisms occurring during or shortly after core hydrogen burning and is also lower than the predicted limit for formation of WR stars through typical single-star mass loss. A number of supernovae also appear to have associated LBV wind nebulae, which argues for an LBV phase shortly before the supernova explosion. This suggests a population of stars in the rough mass range 25–30 $M_\odot$ that undergo severe mass loss late in their evolution, probably due to moving into the LBV eruptive instability strip from the cool side as a result of blue loop evolution or red supergiant or binary-mediated mass loss. Some fraction of these relatively low mass stars could produce WR stars for SN Ib/c progenitors or SN II pec or linear progenitors. At the current time, the numbers of SNe Ib/c produced from this route cannot be predicted from stellar models, which do not include the physics to predict the LBV mass loss, and the observational sample is incomplete. But with better models, we might be able to first determine whether these LBVs are binary induced and second determine what fraction of Wolf-Rayet stars are produced by this class of LBV.

3.9. Gravitational Waves

Observations of gravitational waves can also help constrain the progenitor by providing a direct probe of the angular momentum of the collapsing star. Instabilities in the accretion disk surrounding the black hole and ringing in the forming black hole have both been proposed as sources of gravitational waves (Fryer et al. 2002; see Kobayashi & Mészáros 2003 for a review). Rockefeller et al. (2006) found that, at least for some values of the angular momentum in the collapsing stars, strong spiral instabilities can develop in the disk, producing a gravitational wave signal that is over 10 times stronger than the strongest rapidly rotating normal supernova estimates (consistent with the estimates from Fryer et al. 2002). It is likely that this signal will depend sensitively on the angular momentum of the collapsing star, and it can be used to constrain the rotation rates of collapse progenitors. However, if the signal is as weak as Rockefeller et al. (2006) predict, it is unlikely that we will have a detection anytime soon. Van Putten (2005) has argued that the black hole spin (with its enormous reservoir of energy) can couple to the disk, producing strong instabilities that predict a signal that should make many GRBs easily detectable by advanced Laser Interferometer Gravitational-Wave Observatory (LIGO). If this source is correct, the GW signal can easily be used to constrain progenitor angular momenta. Gravitational wave observations will first determine which of these sources dominate the gravitational wave signal from collapsars. Once the source is determined, we can then use gravitational wave observations to constrain the progenitor.

4. SUMMARY

Since the first discovery of the optical counterpart to a GRB, there has been a wealth of data pointing toward a massive star origin of GRBs. The collapsar engine, invoking the collapse of such massive stars down to a black hole, has become the favored engine behind long-duration gamma-ray bursts. Although progenitors of this engine have been studied for nearly a decade, the list of possible progenitors is still large.

We have reviewed many of the observations that may constrain the nature of the progenitor. Although the observations to date have brought increased support for the massive star origin of GRBs, many of these observations are not strong enough to rule out the progenitors. However, there are some strong statements that can be made about the GRB progenitor. The supernovae associated with GRBs that are bright enough to be studied in detail are Type Ic supernovae. If this result is universal, any progenitor model must lose not only its hydrogen envelope but most of its helium envelope as well. But this sample is limited to 2–3 GRBs at the moment, and it is also known that some GRBs are not at all associated with bright supernovae. We also know that GRBs are even more clustered than their supernova counterparts. That is, they occur most often in the brightest parts of bright galaxies. This may just be an indication that these systems only arise from the most massive stars, but better statistics may argue that certain progenitors must take advantage of cluster environments. GRBs occur in environments with a range of metallicities from 1/100th solar to solar. The mean metallicity may be as high as $\frac{1}{3}-\frac{1}{2}$ solar. This places strong constraints on single-star models. Finally, a potentially strong constraint on the progenitor is the nature of the surrounding environment. A number of long-duration GRB progenitors require ejection of stellar material in a strong wind for quite some time prior to collapse. Current results suggest that the circumprogenitor environment has a free-streaming wind only out to 1 pc; beyond that, the bulk of GRBs appear to have constant density profiles. If such a result can be solidified, it places strong constraints on the GRB progenitor.

In this review, we have discussed many of the current collapsar progenitors and their observational properties. At this time, two single-star progenitor models exist: the classic single-star scenario in which the star loses its hydrogen envelope through winds and the mixing single-star scenario in which the star is able to mix sufficiently well to burn its hydrogen into helium. Both of these single-star models have made strong predictions about the metallicity requirements of the progenitor. If taken at face value, both these scenarios can be ruled out as sole progenitors of GRBs on metallicity requirements alone. These progenitors also do not fit the surrounding environment extremely well, and also produce primarily He-rich (Type Ib) or even H-rich (Type II) supernovae associated with GRBs. These single models clearly do not fit the existing data very well.

A large number of binary progenitor models exist. These models tend to fit the metallicity constraints well. Indeed, if we restrict ourselves to the robust observational constraints, all of these progenitor scenarios can match the existing data. Some progenitor scenarios also may fit the current data taken at face value (assuming all constraints are robust) on the associated supernova, surrounding environment, and peaked clustering of GRBs. However, very few progenitor scenarios fit all of these constraints without some tweaking. There are obvious tweaks, e.g., arguments why only a subset of these progenitors (that subset that matches the strict interpretation of the data constraints) will produce GRBs. These scenarios will be differentiated as the statistics in the current observations become stronger. The current ranking of the various progenitors when compared to the observations is summarized in Table 5.

Studying the progenitors of Type Ib/c supernovae may also provide some insight into the progenitors of GRBs. As with GRBs, when taken at face value, current single-star stellar evolution models cannot produce all normal Type Ib/c supernovae. In fact, the simulations by Heger et al. (2003) argue that at solar metallicity, single stars produce virtually no normal Type Ib/c supernovae. This argues strongly that many Type Ib/c supernovae are produced in binaries. Given the high binary fraction of massive stars, this is to be expected, and it is unlikely that we will understand these supernovae well until binary effects are added to stellar evolution codes.

With the existing robust constraints, it is unlikely that single-

TABLE 5
THEORY VERSUS OBSERVATION

Progenitor	Rate	Associated Supernova	Metallicity	Surrounding Environment	Host Morphology	Distribution
Classic single	T	s	s	S	T	S
Mixing single	T	s	s	S	T	S
Classic binary	T	t	T	t	T	S
Tidal binary	T	t	T	t	T	S
Brown merger	T	t	T	t	T	S
Explosive ejection	T	T	T	T	T	S
He merger	T	t	T	S	T	S
He case C	T	t	T	T	T	S
Cluster	T	t	T	t	T	T

NOTES.—We rank the different scenarios by whether they pass the strong constraint and the trend (T) in the observations, the strong constraint and the trend with a modification or by using a subset of the progenitor class (t), the strong constraint only (S), and the strong constraint only with modifications (s). If the constraint is not strong and the progenitor does not fit the trend, we use "S". These values are not set in stone. Most rankings require much more detailed calculations to confirm.

star models can produce all GRBs. As the data get better, the limitations on single-star models will become more strict. In addition, the data have the potential to differentiate the currently proposed binary progenitors. As we focus in on a progenitor scenario, the metallicity measurements of these GRBs may well teach us a lot about stellar evolution. But for this to work, we must not only obtain better observational statistics; we have to refine our theoretical understanding of these progenitors. This requires a better physical understanding of the uncertainties in stellar evolution and the effects of binaries and the engine behind GRBs. It is now within our computational reach to understand mass loss, convection, and magnetic fields in a rotating star, binary mass transfer, and common-envelope evolution much better than our current parameterized models allow. This combined theoretical and observational work has the potential, in the next two decades, to truly determine the GRB generation.

5. DEFINITIONS

Case A, B, C mass transfer.—Close binary systems can undergo mass transfer when one of the stars overfills its Roche radius. The "case" of this mass transfer is defined by the phase in the star's life during which this mass transfer occurs: case A, during main sequence; case B, after hydrogen burning but before helium ignition; and case C, after helium ignition.

Collapsar.—The explosive engine that is powered by the collapse of a massive star down to the black hole. The energy is derived from the potential energy released as a disk around this black hole accretes onto the black hole. This energy may be converted through neutrinos and their subsequent annihilation or through magnetic fields produced in the disk (Narayan et al. 1992, although see Fryer & Mészáros 2003). All but one of the progenitor scenarios discussed in this review produce collapsars, that is, they produce a rapidly spinning star that later collapses. A similar progenitor scenario, the "helium-merger" scenario (the merger of a compact object with a helium star), is slightly different in that the compact remnant can be formed long before the burst. Nevertheless, it produces conditions similar to those seen in the collapsar engine, and it is often lumped into the collapsar category.

Common-envelope evolution.—During mass transfer, it is possible that the matter overfilling the Roche radius accretes onto the companion star faster than it can be incorporated into the companion star or ejected from the system. This material quickly forms an atmosphere, or envelope, that surrounds both stars in the binary. This "common-envelope" phase leads to the rapid contraction of the binary separation as tidal and viscous forces remove angular momentum from the binary orbit.

Hypernova.—Hypernovae are a peculiar class of supernovae defined observationally by the broad lines in their spectra. This can be caused by either large explosion energies (a few times 10^{51} ergs), low-mass ejecta, or large asymmetries. GRBs are likely to produce supernovae in this subclass.

Supernova type.—Supernova types are determined by observational features. Type I and II supernovae are distinguished by the presence of hydrogen lines (Type I have no hydrogen lines, Type II have hydrogen lines). Type Ia are characterized by a deep silicon II absorption line, which is weak or missing in Type Ib/c supernovae. Type Ib supernovae have He I lines, which are absent in Type Ic supernovae. It is believed that Type Ib/c and II supernovae all arise from the collapse of a massive star.

GRB type.—GRBs are classified by their duration and the hardness of their spectra. The two primary classes are long (>1–3 s) hard bursts and short (<1 s), soft bursts. There may be a third class of short, soft bursts (see Horvath et al. 2006 and references therein).

This project marks the culmination of many discussions held at a workshop on the GRB/SN connection at the KITP attended by nearly all of the authors, and we are grateful for the environment set up at the KITP that allowed these discussions and this collaboration. As such, this work is supported by the National Science Foundation under grant PHY 05-51164. It

was also funded in part under the auspices of the US Department of Energy and supported by its contract W-7405-ENG-36 to Los Alamos National Laboratory, and by NASA grant SWIF03-0047.

REFERENCES

Barth, A. J., et al. 2003, ApJ, 584, L47
Belczynski, K., Bulik, T., Heger, A., & Fryer, C. L. 2007, ApJ, 664, 986
Bethe, H. A., & Brown, G. E. 1998, ApJ, 506, 780
Branch, D., & Nomoto, K. 1986, A&A, 164, L13
Cappellaro, E., Evans, R., & Turatto, M. 1999, A&A, 351, 459
Cappellaro, E., et al. 2005, A&A, 430, 83
Castor, J., McCray, R., & Weaver, R. 1975, ApJ, 200, L107
Castro, S., Galama, T. J., Harrison, F. A., Holtzman, J. A., Bloom, J. S., Djorgovski, S. G., & Kulkarni, S. R. 2003, ApJ, 586, 128
Chen, H.-W., Prochaska, J. X., Bloom, J. S., Ramirez-Ruiz, E., Dessauges-Zavadsky, M., & Foley, R. J. 2007, ApJ, 663, 420
Chen, H.-W., Prochaska, J. X., Bloom, J. S., & Thompson, I. B. 2005, ApJ, 634, L25
Chevalier, R. A., Li, Z.-Y., & Fransson, C. 2004, ApJ, 606, 369
Chin, Y. N., & Huang, Y. L. 1994, Nature, 371, 398
Christensen, L., Hjorth, J., & Gorosabel, J. 2004, A&A, 425, 913
Conselice, C. J., Chapman, S. C., & Windhorst, R. A. 2003, ApJ, 596, L5
Conselice, C. J., et al. 2005, ApJ, 633, 29
Dahlen, T., et al. 2004, ApJ, 613, 189
Della Valle, M., et al. 2006, Nature, 444, 1050
Deng, J., Tominaga, N., Mazzali, P. A., Maeda, K., & Nomoto, K. 2005, ApJ, 624, 898
De Pasquale, M., et al. 2006, A&A, 455, 813
Di Matteo, T., Perna, R., & Narayan, R. 2002, ApJ, 579, 706
Eldridge, J. J., & Vink, J. S. 2006, A&A, 452, 295
Filippenko, A. V. 1997, ARA&A, 35, 309
Firmani, C., Avila-Reese, V., Ghisellini, G., & Tutukov, A. V. 2004, ApJ, 611, 1033
Fruchter, A. S., et al. 2006, Nature, 441, 463
Fryer, C. L. 1999, ApJ, 522, 413
———. 2003, Int. J. Mod. Phys. D, 12, 1795
———. 2006, NewA Rev., 50, 492
Fryer, C. L., Burrows, A., & Benz, W. 1998, ApJ, 496, 333
Fryer, C. L., & Heger, A. 2000, ApJ, 541, 1033
———. 2005, ApJ, 623, 302
Fryer, C. L., Holz, D. E., & Hughes, S. A. 2002, ApJ, 565, 430
Fryer, C. L., Hungerford, A. L., & Young, P. A. 2007, ApJ, 662, L55
Fryer, C. L., & Kalogera, V. 2001, ApJ, 554, 548
Fryer, C. L., & Mészáros, P. 2003, ApJ, 588, L25
Fryer, C. L., & Woosley, S. E. 1998, ApJ, 502, L9
Fryer, C. L., Woosley, S. E., & Hartmann, D. 1999, ApJ, 526, 152
Fryer, C. L., Young, P. A., & Hungerford, A. L. 2006a, ApJ, 650, 1028
Fryer, C. L., Young, P. A., & Rockefeller, G. 2006b, ApJ, 647, 1269
Fynbo, J. P. U., et al. 2006, Nature, 444, 1047
Gal-Yam, A., et al. 2006a, ApJ, 639, 331
———. 2006b, Nature, 444, 1053
Garcia-Segura, G., Langer, N., & Mac Low, M.-M. 1996, A&A, 316, 133
Gehrels, N., et al. 2006, Nature, 444, 1044
Guetta, D., & Della Valle, M. 2007, ApJ, 657, L73
Hadfield, L. J., & Crowther, P. A. 2006, MNRAS, 368, 1822
Harkness, R. P., et al. 1987, ApJ, 317, 355
Heger, A., Fryer, C. L., Woosley, S. E., Langer, N., & Hartmann, D. H. 2003, ApJ, 591, 288
Hirschi, R., Meynet, G., & Maeder, A. 2004, A&A, 425, 649
———. 2005, A&A, 443, 581
Horvath, I., Ryde, F., Balazs, L. G., Bagoly, Z., & Meszaros, A. 2006, in AIP Conf. Proc. 836, Gamma-Ray Bursts in the *Swift* Era, ed. S. S. Holt, N. Gehrels, & J. A. Nousek (Melville: AIP), 125
Ivanova, N., & Podsiadlowski, P. 2003, in From Twilight to Highlight: the Physics of Supernovae, ed. W. Hillebrandt & B. Leibundgut (Berlin: Springer), 19
Iwamoto, K., et al. 1998, Nature, 395, 672
Izzard, R. G., Ramirez-Ruiz, E., & Tout, C. A. 2004, MNRAS, 348, 1215
Jakobsson, P., et al. 2006, A&A, 460, L13
Kewley, L. J., Brown, W. R., Geller, M. J., Kenyon, S. J., & Kurtz, M. J. 2007, AJ, 133, 882
Kobayashi, S., & Mészáros, P. 2003, ApJ, 589, 861
Kobulnicky, C. 2005, in AIP Conf. Proc. 783, The Evolution of Starbursts, ed. S. Hüttemeister (Melville: AIP), 381
Kobulnicky, H. A., & Fryer, C. L. 2007, ApJ, 670, 747
Kotake, K., Yamada, S., & Sato, K. 2003, ApJ, 595, 304
Kudritzki, R. 2000, in The First Stars, ed. A. Weiss, T. G. Abel, & V. Hill (Berlin: Springer), 127
Kumar, P., & Panaitescu, A. 2000, ApJ, 541, L9
Lamers, H. J. G. L. M., & Cassinelli, J. P. 1999, Introduction to Stellar Winds (Cambridge: Cambridge Univ. Press)
Li, W., Wang, X., Van Dyk, S. D., Cuillandre, J.-C., Foley, R. J., & Filippenko, A. V. 2007, ApJ, 661, 1013
Limongi, M., & Chieffi, A. 2006, ApJ, 647, 483
Lucy, L. B. 1991, ApJ, 383, 308
Maeda, K., Mazzali, P. A., & Nomoto, K. 2006, ApJ, 645, 1331
Maeda, K., et al. 2007, ApJ, 666, 1069
Matsubayashi, T., Yamazaki, R., Yonetoku, D., Murakami, T., & Ebisuzaki, T. 2005, Prog. Theor. Phys., 114, 983
Maund, J. R., Smartt, S. J., Kudritzki, R. P., Podsiadlowski, P., & Gilmore, G. F. 2004, Nature, 427, 129
Mazzali, P. A., & Lucy, L. B. 1998, MNRAS, 295, 428
Mazzali, P. A., et al. 2003, ApJ, 599, L95
———. 2006, ApJ, 645, 1323
Meakin, C. A., & Arnett, D. 2006, ApJ, L53
Mészáros, P., & Rees, M. 1997, ApJ, 476, 232
Meynet, G., & Maeder, A. 2007, A&A, 464, L11
Mirabel, I. F., Mignani, R., Rodrigues, I., Combi, J. A., Rodríguez, L. F., & Guglielmetti, F. 2002, A&A, 395, 595
Modjaz, M., Kewley, L., Kirshner, R. P., Stanek, K. Z., Challis, P., Garnavich, P. M., Greene, J. E., & Prieto, J. L. 2007, AJ, submitted (astro-ph/0701246)
Mokiem, R. 2006, Ph.D. thesis, Univ. Amsterdam
Narayan, R., Paczyński, B., & Piran, T. 1992, ApJ, 395, L83
Nemiroff, R. J. 1994, Comments Astrophys., 17, 189
Nomoto, K. 2005, in Supernovae: One Millennium After SN1006, 26th Meeting of the IAU, Joint Discussion 9, No. 8
Nomoto, K., Iwamoto, K., & Suzuki, T. 1995a, Phys. Rep., 256, 173
Nomoto, K., Iwamoto, K., Yamaoka, H., Suzuki, T., Pols, O. R., van den Heuvel, E. P. J., & Höflich, P. 1995b, Ann. NY Acad. Sci., 759, 360
Nomoto, K., Maeda, K., Tominaga, N., Ohkubo, T., Deng, J., & Mazzali, P. A. 2005, Ap&SS, 298, 81

Nomoto, K., Maeda, K., Umeda, H., Ohkubo, T., Deng, J., & Mazzali, P. 2003, in IAU Symp. 212, A Massive Star Odyssey, from Main Sequence to Supernova, ed. V. D. Hucht et al. (San Francisco: ASP), 395
Nomoto, K., Suzuki, T., Shigeyama, T., Kumagai, S., Yamaoka, H., & Saio, H. 1993, Nature, 364, 507
Nomoto, K., Tominaga, N., Tanaka, M., Maeda, K., Suzuki, T., Deng, J. S., & Mazzali, P. A. 2006a, Nuovo Cimento B, 121, 1207
Nomoto, K., Tominaga, N., Umeda, H., Kobayashi, C., & Maeda, K. 2006b, Nucl. Phys. A, 777, 424
Nomoto, K., Yamaoka, H., Pols, O. R., van den Heuvel, E. P. J., Iwamoto, K., Kumagai, S., & Shigeyama, T. 1994, Nature, 371, 227
Nousek, J. A., et al. 2006, ApJ, 642, 389
Nugis, T., & Lamers, H. J. G. L. M. 2000, A&A, 360, 227
Ofek, E. O., et al. 2007, ApJ, 662, 1129
Paczyński, B. 1998, in AIP Conf. Proc. 428, The Gamma-Ray Bursts: 4th Huntsville Symp., ed. C. A. Meegan, R. D. Preece, & T. M. Koshut (Woodbury: AIP), 783
Panaitescu, A. 2005, MNRAS, 363, 1409
Panaitescu, A., & Kumar, P. 2003, ApJ, 592, 390
Panaitescu, A., Mészáros, P., Gehrels, N., Burrows, D., & Nousek, J. 2006, MNRAS, 366, 1357
Pian, E., et al. 2006, Nature, 442, 1011
Podsiadlowski, P., Hsu, J. J. L., Joss, P. C., & Ross, R. R. 1993, Nature, 364, 509
Podsiadlowski, P., Ivanova, N., Justham, S., & Rappaport, S. 2007, MNRAS, submitted
Podsiadlowski, P., Joss, P. C., & Hsu, J. J. L. 1992, ApJ, 391, 246
Podsiadlowski, P., Joss, P. C., & Rappaport, S. 1990, A&A, 227, L9
Podsiadlowski, P., Mazzali, P. A., Nomoto, K., Lazzati, D., & Cappellaro, E. 2004, ApJ, 607, L17
Portegies-Zwart, S. F., Dewi, J., & Maccarone, T. 2005, Ap&SS, 300, 247
Prantzos, N., & Boissier, S. 2003, A&A, 406, 259
Prieto, J. L., Stanek, J. L., & Beacom, J. F. 2007, ApJ, in press (astro-ph/0707.0690)
Prochaska, J. X. 2003, ApJ, 582, 49
———. 2006, ApJ, 650, 272
Prochaska, J. X., Bloom, J. S., Chen, H.-W., Hurley, K. C., Melbourne, J., Dressler, A., Graham, J. R., Osip, D. J., & Vacca, W. D. 2004, ApJ, 611, 200
Prochaska, J. X., Chen, H.-W., & Bloom, J. S. 2006, ApJ, 648, 95
Richardson, D., Branch, D., & Baron, E. 2006, AJ, 131, 2233
Rockefeller, G., Fryer, C. L., & Li, H. 2006, ApJ, submitted (astro-ph/0608028)
Ryder, S. D., Murrowood, C. E., & Stathakis, R. A. 2006, MNRAS, 369, L32
Saio, H., Nomoto, K., & Kato, M. 1988a, ApJ, 331, 388
———. 1988b, Nature, 334, 508
Sato, G., et al. 2007, ApJ, 657, 359
Sauer, D. N., Mazzali, P. A., Deng, J., Valenti, S., Nomoto, K., & Filippenko, A. V. 2006, MNRAS, 369, 1939
Savaglio, S., Fall, S. M., & Fiore, F. 2003, ApJ, 585, 638
Schaefer, B., et al. 2003, ApJ, 588, 387
Shigeyama, T., Nomoto, K., Tsujimoto, T., & Hashimoto, M. 1990, ApJ, 361, L23
Shimizu, T., Yamada, S., & Sato, K. 1994, ApJ, 432, L119
Smith, N., Vink, J. S., & de Koter, A. 2004, ApJ, 615, 475
Soderberg, A. M., Frail, D. A., & Wieringa, M. H. 2004, ApJ, 607, L13
Soderberg, A. M., Nakar, E., Berger, E., & Kulkarni, S. R. 2006a, ApJ, 638, 930
Soderberg, A. M., et al. 2006b, ApJ, 636, 391
Sollerman, J., Östlin, G., Fynbo, J. P. U., Hjorth, J., Fruchter, A., & Pedersen, K. 2005, NewA, 11, 103
Spruit, H. C. 2002, A&A, 381, 923
Stanek, K. Z., Gnedin, O. Y., Beacom, J. F., Gould, A. P., Johnson, J. A., Kollmeier, J. A., Modjaz, M., Pinsonneault, M. H., Pogge, R., & Weinberg, D. H. 2006, Acta Astron., 56, 333
Starling, R. L. C., Wijers, R. A. M. J., Wiersema, K., Rol, E., Curran, P., Kouveliotou, C., van der Horst, A. J., & Heemskerk, M. H. M. 2007, ApJ, 661, 787
Stephenson, F. R., & Clark, D. H. 1976, Sci. Am., 234, 100
Taubenberger, S., et al. 2006, MNRAS, 371, 1459
Tutukov, A. V., & Cherepaschuck, A. M. 2004, Astron. Rep., 48, 39
van den Heuvel, E. P. J., & Yoon, S.-C. 2006, presentation at KITP, http://online.itp.ucsb.edu/online/grb06/vandenheuvel/
———. 2007, Ap&SS, submitted (arXiv: 0704.0659)
van Marle, A. J., Langer, N., & Garcia-Segura, G. 2005, A&A, 444, 837
van Putten, M. H. P. M. 2005, Gravitational Radiation, Luminous Black Holes and Gamma-Ray Burst Supernovae (Cambridge: Cambridge Univ. Press)
Vinki, J. S., de Koter, A. 2005, A&A, 442, 587
Vreeswijk, P. M., et al. 2004, A&A, 419, 927
———. 2007, A&A, 468, 83
Wainwright, C., Berger, E., & Penprase, B. E. 2007, ApJ, 657, 367
Wheeler, J. C., et al. 1987, ApJ, 313, L69
Wijers, R. 2001, in Gamma-Ray Bursts in the Afterglow Era, ed. E. Costa, F. Frontera, & J. Jorth (Berlin: Springer), 306
Willingale, R., et al. 2006, ApJ, submitted (astro-ph/0612031)
Winkler, P. F., Kirshner, R. P., Hughes, J. P., & Heathcote, S. R. 1989, Nature, 337, 48
Wolf, C., & Podsiadlowski, P. 2007, MNRAS, 375, 1049
Woosley, S. E. 1993, ApJ, 405, 273
Woosley, S. E., Eastman, R. G., Weaver, T. A., & Pinto, P. A. 1994, ApJ, 429, 300
Woosley, S. E., & Heger, A. 2006, ApJ, 637, 914
Woosley, S. E., Heger, A., & Weaver, T. A. 2002, Rev. Mod. Phys., 74, 1015
Woosley, S. E., & Weaver, T. A. 1995, ApJS, 101, 181
Yoon, S.-C., & Langer, N. 2005, A&A, 443, 643
Yoon, S.-C., Langer, N., & Norman, C. 2006, A&A, 460, 199
Young, P. A., Meakin, C., Arnett, D., & Fryer, C. L. 2005, ApJ, 629, L101
Young, P. A., et al. 2006, ApJ, 640, 891
Zhang, B., & Mészáros, P. 2004, Int. J. Mod. Phys. A, 19, 2385
Zhang, B., et al. 2006, ApJ, 642, 354